Mon. Not. R. astr. Soc. (1992) **258**, 1–22

The Edinburgh–Durham Southern Galaxy Catalogue – IV. The Cluster Catalogue

S. L. Lumsden,[1,2]★ R. C. Nichol,[3] C. A. Collins[2] and L. Guzzo[4]

[1] *Astrophysics Group, Imperial College of Science, Technology & Medicine, Blackett Laboratories, Prince Consort Road, London SW7 2BZ*
[2] *Royal Observatory, Blackford Hill, Edinburgh EH9 3HJ*
[3] *Department of Astronomy, University of Edinburgh, Blackford Hill, Edinburgh EH9 3HJ*
[4] *Osservatorio Astronomico di Brera, Sedi di Merate, Via Bianchi 46, I-22055 Merate, Italy*

Accepted 1992 February 19. Received 1992 January 29; in original form 1991 November 5

SUMMARY

We present the Edinburgh–Durham Cluster Catalogue (EDCC). This is the first machine-based, objectively selected sample of clusters of galaxies. It consists of 737 clusters or groups of all richnesses, over 0.5 sr of sky, centred on the South Galactic Pole (SGP). The primary galaxy data set for the cluster survey is the Edinburgh–Durham Southern Galaxy Catalogue (EDSGC). The EDCC was constructed using an automatic peak-finding algorithm and is complete to $m_{10}(b_j) = 18.75$. In a comparison with the Abell clusters in the same region, we detect 80 per cent of their rich clusters nominally brighter than our completion limit in addition to many new systems. This suggests that the EDCC is 90 per cent complete for Abell-type clusters. We also conclude that the Abell magnitude system is biased towards bright magnitudes for most of their clusters, and that their richness estimates are prone to a larger uncertainty than they suggest. The EDCC therefore supersedes the Abell catalogue as a data base for statistical studies of cluster properties.

Key words: catalogues – galaxies: clustering.

1 MOTIVATION

Clusters of galaxies provide a powerful probe of the form and evolution of structure on large scales and have been used in many diverse areas of cosmological study. For example, clusters provide a measure of large-scale clustering, both for the spatial correlation function (Bahcall & Soneira 1983) and for the angular correlation function (Couchman, McGill & Olowin 1989). The luminosity function can be used to provide evidence for the evolution of clusters. Attempts have been made to model the luminosity function of clusters in terms of some universal function (e.g. Abell 1962; Schechter & Press 1976; Dressler 1978; Lugger 1986; Colless 1989). Clusters also provide a powerful test of the gravitational lensing hypothesis (see, for example, Ellis 1990), and hence may be useful as an unbiased source of serendipitous high-redshift galaxies. Furthermore, clusters have been used in studies of streaming motions (see, for example, Aaronson *et al.* 1986 and Lynden-Bell *et al.* 1988).

★Present address: Astrophysics Department, University of Oxford, Keble Road, Oxford OX1 3RH.

There are a number of existing cluster catalogues in the literature. The most widely used is the Abell catalogue (Abell 1958) and its southern counterpart (Abell, Corwin & Olowin 1989, hereafter ACO). Together these consist of an all-sky cluster sample supposed to be at redshifts less than 0.2, selected from Palomar (UK Schmidt for ACO) plates. Other catalogues include the Zwicky *et al.* (1961–68) catalogue of clusters and galaxies and Shectman's (1985) analysis of the Shane & Wirtanen (1967) counts from the Palomar survey plates.

The main problem with all these catalogues is that they are based on data gathered from visual inspection of the galaxy distribution with different (and largely unquantifiable) selection procedures giving rise to heterogeneous catalogues. It has been recognized for some time that the intrinsically subjective nature of the Abell catalogue gives rise to severe problems in homogeneity and statistical completeness (Postman, Geller & Huchra 1986). Additional problems arising from projection effects within the Abell catalogue render the clustering results of Bahcall & Soneira (1983) very uncertain (Sutherland 1988). Many of these problems can be solved or at least quantified with an objective, machine-based catalogue. Such a data base, with accurate photometry, would prove an invaluable aid in clarifying existing uncertainties and allow substantial progress to be made in many areas of cluster research.

The main purpose of this paper is to present the first large-scale automated cluster survey using a combination of a modified Shectman approach with a modified Abell analysis. From this we determine the statistical completeness of the Abell catalogue. The structure of this paper is as follows: in Section 2, we discuss the construction of the EDCC; in Section 3, we present and describe the catalogue; in Section 4, we compare it to the Abell clusters in the same region and hence find a measure of the reliability of the Abell catalogue; and in Section 5, we summarize the results of this study.

2 CONSTRUCTION OF THE CATALOGUE

2.1 The galaxy data

The source of our galaxy data is the Edinburgh–Durham Southern Galaxy Catalogue (hereafter EDSGC: Heydon-Dumbleton, Collins & MacGillivray 1989, Paper 2), which consists of COSMOS scans of 60 UK Schmidt survey plates. The EDSGC covers 0.5 sr, centred on the South Galactic Pole. Accurate calibration and star–galaxy separation have resulted in a catalogue that is 95 per cent complete to $b_{\mathrm{j}} \sim 20.5$ with less than 10 per cent stellar contamination, and a plate-to-plate zero-point variation of $\Delta m \sim 0.05$. The COSMOS image analysis package (Thanisch, McNally & Robin 1984; Beard, MacGillivray & Thanisch 1990) also contains a powerful deblending routine which we use to discriminate between the different galaxies in rich cluster cores. This is vital for our purposes since an underestimate of the number of galaxies in a rich compact core could easily result in that cluster being overlooked. The EDSGC is therefore an ideal tool for many large-scale cosmological survey projects.

2.2 Finding candidate clusters

In this paper we utilize a similar approach to that of Abell in classifying clusters since our aim is to test the reliability of the Abell catalogue. We adopted a method of finding cluster candidates independent of any presumed cluster model and imposed the Abell classification at a later stage. We intend to consider the same candidate clusters in terms of non-Abell parameters in future papers. There are two well-established mechanisms for carrying out this task. The one we used involves binning the galaxy data, and is modified from the work of Shectman (1985). The alternative is to use a percolation analysis. We decided not to use this method since it can in principle merge nearby candidate objects into a single structure. Consideration of the computer time involved also favours the binning method.

The catalogue was binned into equal-area square bins on a true sky projection. The bin size was chosen such that the mean number of galaxies per bin was ~ 1. This procedure was carried out three times, for different magnitude limits; the actual limits and bin sizes used are given in Table 1. Each selection gave rise to a different set of candidates, although, as might be expected, there were large overlaps.

Once the data were binned, they were lightly smoothed with a Shectman (1985) filter to produce a 'Shectman' frame. This filter has the weights

$$\begin{matrix} \frac{1}{16} & \frac{1}{8} & \frac{1}{16} \\ \frac{1}{8} & \frac{1}{4} & \frac{1}{8} \\ \frac{1}{16} & \frac{1}{8} & \frac{1}{16}. \end{matrix}$$

The Shectman filter was chosen since it is effectively a Gaussian filter, and hence matches the cluster density profiles well (a point that we make use of again in the Abell analysis). Over-smoothing the data (using a top-hat filter for example) reduces the likelihood of detecting real small-scale structures, and not smoothing at all would make location of a peak dependent on its location with respect to the bin. Light smoothing reduces binning noise, ensuring that a true peak is located irrespective of where it lay in the original bins. The validity of this latter point will be discussed further in Section 2.5 when the errors in the catalogue are considered.

Shectman searched for peaks above a global threshold. However, since the EDSGC gives only a two-dimensional representation of the actual galaxy density on the sky, it is impossible to find all clusters in this way. A single threshold will find all clusters, however poor, in a region of generally high galaxy density and, conversely, miss those, however rich, in regions of low galaxy density. In order to overcome this problem, the large-scale baseline was removed by following the background projected density (Dodds & MacGillivray 1986). This background or 'sky' frame was calculated by smoothing the 'Shectman' frame using a square, mean filter of width between 1° and 2°. Tests showed that the clusters selected were actually quite resilient to the exact form of this 'sky' frame. Changing the scale on which the background is smoothed (within the range 40 arcmin to 3°), and hence changing the effective background level, causes less than a 10 per cent change in the final candidate centres. Most of the candidates that were sensitive to this change were found to be 'noise'.

The 'sky' frame was subtracted from the 'Shectman' frame. An analysis package similar to the COSMOS image analyser (Thanisch, McNally & Robin 1984; Beard, MacGillivray & Thanisch 1990) was used to find pixels above a given threshold in this background-subtracted image. The threshold was set according to the values given in Table 1. These values were set empirically as a compromise between rejecting real clusters while keeping the proportion of 'noise'

Table 1. Values used in the binning routines.

run no.	magnitude limit	bin size (arcmin)	threshold (galaxies/bin)	number of cands
1	18.5	8	1.5 ($2.3\sigma, \sigma = 0.65$)	438
2	19.5	5	2.5 ($3.9\sigma, \sigma = 0.64$)	491
3	20.5	3	3 ($4.6\sigma, \sigma = 0.65$)	633

images to a minimum. The threshold varies between runs since the number of such 'noise' images increases as the bin size is decreased. If the threshold was lowered it would be possible to counteract this by including an area cut, but this was found to exclude some genuine distant clusters. Therefore, from experiments on a small area of the data, we chose thresholds which gave minimum contamination without discarding any of the clusters that we had previously detected by eye. Only 5 per cent of the objects detected definitely proved not to be clusters or groups of galaxies on a further visual inspection.

Thresholding the data is not sufficient to find all true density peaks. Clearly, neighbouring peaks can lie above the same threshold. We therefore deblended the data in density space to search for the true peaks and the saddle points between them. Failure to do this would have led to nearby groups of clusters being considered as a single unit. Applying an Abell classification to that single unit would give misleading results, since we would have no further information that there was in fact more than one peak in the density distribution at that position. Deblending before applying the Abell mechanism allows us to note that there are two or more overlapping Abell radii for the candidates, and hence to correct the counts again at a later point in the analysis. This is also the reason that we decided against using a percolation method for selecting candidate clusters. This helps to reduce the problem of projection effects which have been noted as a common occurrence in the Abell (1958) catalogue (Lucey 1983; Sutherland 1988). Since the background-subtracted frame is analogous to a galaxy density, linear thresholding was used in contrast to the COSMOS software used to deblend merged galaxy/star images in the construction of the EDSGC. We used 20 thresholds, starting at the thresholds given in Table 1 and ending at the peak in the actual structure. The other major difference between the procedure applied here and the COSMOS package was that each pixel was allocated to only one cluster. This is justified for two reasons. First, there were very few instances in which pixels were equally shared. Secondly, since we later imposed the Abell classification and then deblended again, the small richness errors arising at this stage from this simplification were irrelevant. For every candidate, the locations of all pixels belonging to that object (which by definition must be connected), and the EDSGC catalogue information on all the galaxies within those pixels were stored for future use. The numbers of candidate clusters found for the different bin sizes are given in Table 1.

2.3 The Abell analysis

The methods outlined by Abell (1958) are valuable for three reasons. They provide an opportunity to place the EDCC within a recognized framework, a method of giving additional information over that presented by the pseudo-'Shectman' analysis given above, and also allow us to make a direct comparison between our catalogue and that of Abell.

The candidate cluster centres were taken as initial centroids for the true Abell cluster. The magnitude of the tenth brightest galaxy, m_{10}, was taken from the list of galaxies contained within the pixels. This magnitude was converted into an Abell radius, θ_A, using the formula given by ACO; the Abell radius is the angle subtended on the sky by a circle of radius $1.5h^{-1}$ Mpc at the cluster, ignoring cosmological corrections.

$$\theta_A = \arctan\left(\frac{150}{cz}\right), \tag{1a}$$

where cz is given by equation (11) of ACO (the well-known m_{10}–logcz relation), and a correction of

$$b_j - V = 0.77 \tag{1b}$$

has been made to convert from the EDSGC magnitude system (b_j) to the ACO system (V). This value was obtained from the calibration sequences used in the construction of the EDSGC (Heydon-Dumbleton *et al.* 1989). It should also be noted that the ACO form of the m_{10}–logcz relation is in reasonable agreement with that found by Scaramella *et al.* (1990) for the same clusters and using updated redshifts.

Allowance must be made for the galaxies seen in projection on the cluster before the Abell radius can be calculated. An estimate of the contamination was derived from number counts of all the galaxies in a box of 4° × 4° centred on the original candidate. These counts were then scaled down to the cluster area. The contribution of cluster galaxies to this count on each field is negligible once the counts are scaled down. Calculating the background in this way guards against only using an unrepresentative low-density region, free from clusters (as Abell did), and so should be more reliable. Since the cluster area is a function of m_{10}, this is an iterative process, but in general it converges rapidly. For the clusters presented here, convergence was taken to be the point at which the value of m_{10} was stable to within 1 per cent between iterations.

For very distant clusters, it was sometimes the case that the 'true' m_{10} actually lay beyond the EDSGC magnitude limit. In that case, the candidate was discarded. Similarly, if the centroid moved in the iteration by more than a quarter of its initial Abell radius it was discarded (since such a cluster is likely to be too poor for the iterative process to be stable), and if the value of m_{10} failed to converge within 10 tries it was discarded. In this way 20, 15 and 25 per cent of the candidates from the respective runs were removed from further consideration. The high rejection rate for the smallest bin size was largely due to candidates whose magnitudes lay very near the plate limits, and that for the largest bin size because the low threshold allowed many poor nearby groups to be considered which consequently moved the centroid in the analysis.

The centroid of the cluster was defined by using all the galaxies within the Abell radius since the background should be smooth across these scales. The richness is defined as the number of galaxies in the magnitude range $[m_3, m_3+2]$, as in Abell, also corrected for the background contamination in the same manner that m_{10} was.

2.4 The final catalogue

The next step in the construction of the catalogue was to combine the data from the Abell analyses of each of the three runs using the different initial bin sizes. The first step in this process was to remove duplicate entries from the final list. Any cluster which overlapped with other clusters so that its centroid fell within another's Abell radius was flagged as being a possible duplicate. Any isolated clusters were passed straight into the final catalogue since they required neither merging nor deblending.

We used a two-sided Kolmogorov–Smirnov (KS) test to compare the background-subtracted magnitude distributions for those clusters found to be overlapping. This can also be viewed as comparing the luminosity functions of the two clusters through their apparent magnitude distributions but, crucially, places no constrictions on the form of the distribution. It is also formally independent of the number of objects under consideration (so it is useful for the poorer systems). A more conservative approach would have been to include every cluster from the different runs in the final catalogue, but this ignores the fact that many of the candidates from different runs were clearly the same cluster. The KS test is a relatively weak constraint (see below). Since some of the distinct peaks that we locate may be due to substructure we opted for these relatively loose constraints in combining the three original catalogues.

Where the apparent magnitude distribution was found to be the same, within a given significance level, we accepted these clusters as being the same. The level of significance that we used varied according to the separation of the clusters. This was found empirically on visual inspection of the candidates to be well behaved, whereas using only one threshold gave either too few or too many blends depending on which level of significance was chosen. For those clusters where both the centroids were within each other's Abell radius, clusters had to pass at the 10 per cent level; for those where one centroid was within the other's Abell radius, clusters had to pass at the 20 per cent level; and for those where only the Abell radii overlapped (those which had been grouped through a common third cluster that lay between them for example), the requirement was that the distribution should be the same at the 40 per cent level of significance. To estimate how rigorous these limits were we selected a cluster with a richness of 40, and $m_{10} = 18$, typical of our catalogue, and then varied the magnitude and the effective richness and compared it against itself. A shift in magnitude of 0.2 (roughly a difference in redshift of 0.01), or a change in richness by 60 per cent caused a failure at the 10 per cent level. Therefore substructure on its own is unlikely to cause a failure, and only distinct clusters should be excluded by this test. Correspondingly smaller shifts would cause failure at the stricter levels for those clusters that only partially overlapped.

In cases where more than two clusters overlapped, we ranked them according to the size of their Abell radius. All the clusters were compared with the largest, and those that matched were removed. The remaining set were then compared with the remaining largest cluster in the same manner. This process continued until all the clusters had been allocated to final distinct products. These final products were then reanalysed in order to determine their Abell characteristics. In the actual data set before the KS test was applied there were 425 clusters which existed in only one run, 154 clusters which were found in two distinct runs, 89 triplets in three distinct runs, and 55 other combinations of more than three initial candidates (42 objects consisting of 211 initial candidates) or mergers where more than one of the components came from the same run (as happened for 10 triplets and three pairs). After the KS test, these numbers became 461 singlets, 178 distinct pairs, 93 triplets, and 37 others (29 complex objects consisting of 126 initial candidates and two pairs and six triplets). Only the complex combinations were affected by the KS test since the other groups have virtually the same centres in the different runs, and hence almost exactly the same magnitude distributions. Clearly, from these figures, the test has passed virtually all the clusters it should have, but has discriminated against large complex groupings which were actually blends of distinct clusters. In total, therefore, we reduced the three original runs to a final list of 769 clusters. Information on how many times a given cluster was detected in the individual runs is given in the catalogue (Table 3), from which the reliability of our procedure can be checked.

Finally, this single set of clusters was again checked for overlaps. Where overlaps were found, since the KS test had shown these clusters were distinct, deblending was applied to ensure that every galaxy could only appear in one distinct cluster. 255 clusters in 110 blended groups were treated in this way. This fraction (33 per cent) compares favourably with previous estimates (Lucey 1983) for the Abell catalogue. Only galaxies in the overlaps between clusters were tested, since testing all galaxies in a blended pair usually resulted in all the galaxies in very poor clusters being assigned to the richer system, which was found by visual inspection to be unrealistic. For simplicity, a Gaussian distribution was fitted to the density profile of every cluster in a blend, and the cluster whose Gaussian fit had the largest amplitude at the location of any galaxy was assigned that galaxy. Once all the galaxies had been allocated to clusters, the cluster properties were again reanalysed (since the values of m_3 and m_{10} can change during the deblending process).

2.5 Error estimates

The internal errors in the Abell parameters can be estimated by comparing the output from the three separate runs. We considered those overlapping clusters which passed the KS test to be essentially separate measurements on the same intrinsic cluster. Since there were cases of multiple blends, we used only the nearest clusters from the other two runs to a cluster in a given run (this avoids problems with using clusters which effectively sample largely different areas of the data). The scatter found in this way should give a realistic estimate of the underlying error in the final cluster catalogue. Fig. 1(a) shows a comparison of the derived m_{10}s for all the clusters, Fig. 1(b) that for the m_{10}s when only clusters with more than 30 members were considered and Fig. 1(c) a comparison of the richness values. This information is also summarized in Table 2, where the estimated intrinsic errors in the final catalogue are also given. The average differences between runs for any of the parameters given there were effectively consistent with zero (as can be seen from Fig. 1).

Some fairly obvious points can be made about these scatter plots. The scatter in the value of m_{10} is reduced when only the richer clusters are considered, as would be expected. Also, there appears to be a correlation between the size of the original bin and the final value of the m_{10} in the sense that larger bins give rise to brighter m_{10}s. However, this is less evident in the richer clusters, probably indicating that some of the poorer clusters are not well defined. Note also that the scatter in the brighter magnitudes (m_1, m_3) is larger than in

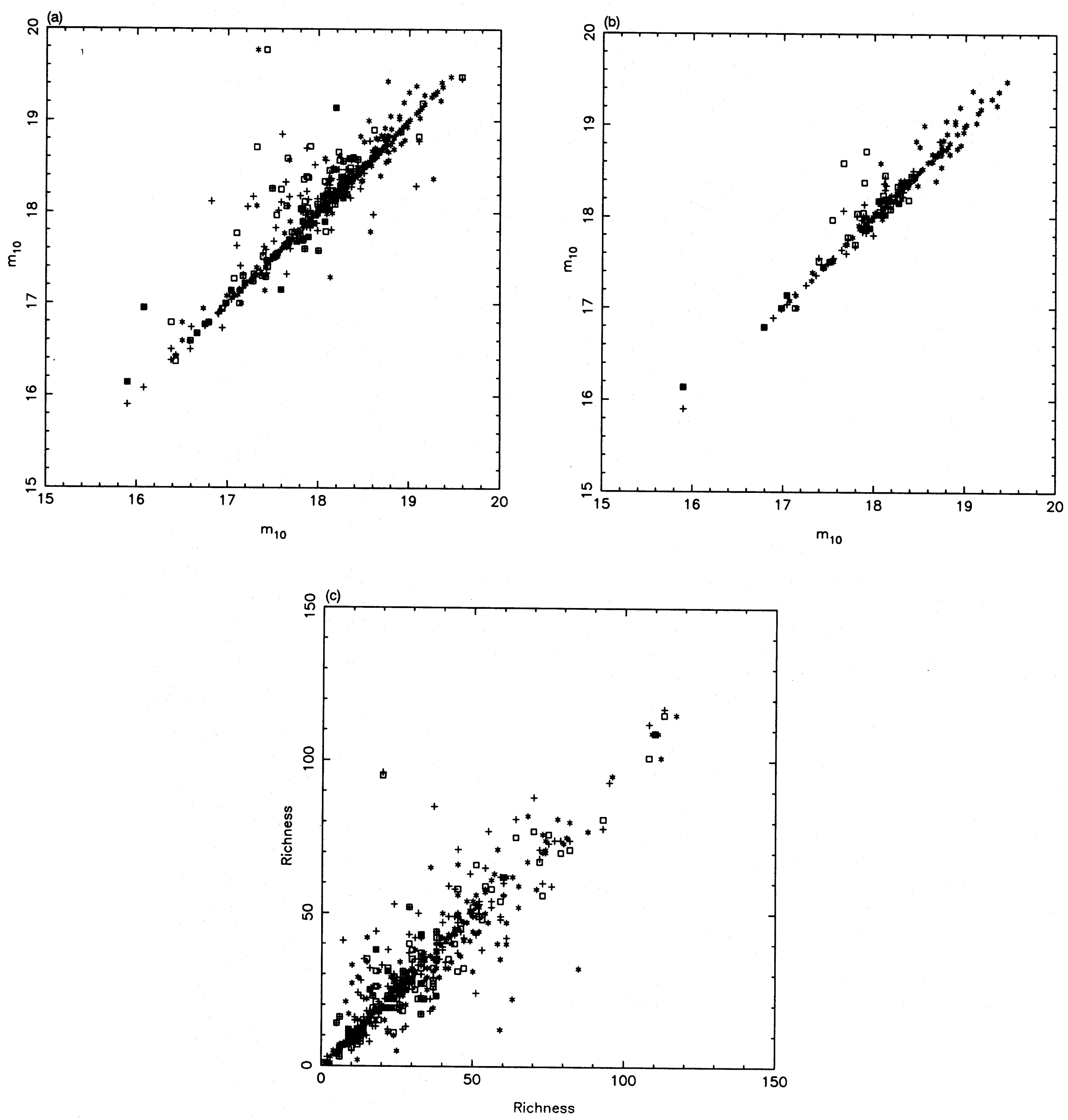

Figure 1. Scatter plots showing the comparison of (a) m_{10} values for all EDCC clusters, (b) m_{10} values for those with more than 30 members, and (c) richness values for all EDCC clusters. Symbols are (+) for run 1 against run 2, (□) for run 1 against run 3, and (*) for run 2 against run 3. In all cases the lower numbered run is on the x-axis.

m_{10}, which would be expected since m_{10} is closer to the peak in the cluster luminosity function (so an error in selecting the actual tenth brightest galaxy is less likely to give rise to a large error in the magnitude). However, the scatter in richness is not reduced if only richer clusters are compared. This is largely due to a coupling between two effects. Overall, the scatter in m_3 is smaller for richer clusters, but the induced richness error is also proportional to the richness itself. For a Schechter-style luminosity function it can be seen that such an error in m_3 leads to an error in the richness that is approximately equal to the product of the number of objects in the cluster and the error in the magnitude (*cf.* Colless 1989, equation 10). Since these two effects almost cancel we would expect the overall scatter for the richness to be approximately the same irrespective of the actual richness, as is observed.

Finally, removing those overlaps where the offset between the centroids is more than 2 arcmin reduces the scatter considerably (see the final entry in Table 2). These errors must represent the irreducible minimum errors within the

EDCC and can be seen to arise from the actual mechanics of the iteration process. Slight shifts in the initial centroid can lead to a slightly different initial value for m_{10}. The iteration procedure ends when the m_{10}s between successive iterations agree to within 1 per cent, so potentially the final magnitudes can differ by 0.1–0.2 mag. Hence, the minimal scatter is consistent with that expected from the iteration procedure.

One other possible source of error was the residual effect of the binning, not adequately accounted for by the Shectman filter. In order to test whether or not residual binning noise played any part in the selection procedure, the bin centres were offset by half a bin width and a reselection made. This error might have been expected to dominate near the edge of the survey for instance, where background subtraction is more uncertain and small shifts in the centroid are more likely to have a correspondingly larger effect. In fact the resulting changes to the various cluster properties were consistent with the minimal measurement errors described above. In addition, the same density peaks were found in both the original and offset data, indicating that any residual effect of the binning was negligible.

3 THE CLUSTER CATALOGUE

Table 3 gives the measured properties for all the clusters in the EDCC. There were 769 clusters remaining after identifying duplicates. No restriction has been made on richness or distance (unlike ACO). The catalogue is based around detecting local peaks in the density distribution. Though the Abell classifications may be questionable (see below) in some cases, there were only a few instances (32 cases) in which the peak in the smoothed data did not appear to correlate with any visible cluster on the plates. Those which were judged to be outright errors are listed separately in Table 4. A computer-readable version of Table 3 is available from the authors on request, as are details of the original separate 'runs'. The table is sorted in right ascension and contains the following information. (1) Sequential EDCC cluster identification numbers. (2) Right ascension and declination (equinox 1950). (3) The magnitude of first, third and tenth brightest members (m_1; m_3; m_{10}). (4) The number of galaxies within the Abell radius between m_3 and m_3+2 *after* the background galaxies have been removed ($n_{\rm clus}$). (5) The number of background galaxies within the same radius to the same magnitude limit ($n_{\rm back}$). The actual original counts within $\theta_{\rm A}$ can be reconstructed from $n_{\rm raw}=n_{\rm clus}+n_{\rm back}$. (6) The Abell radius ($\theta_{\rm A}$) in degrees. (7) Schmidt J survey field number. (8) The number of times the cluster was located in each of the original runs; for example, 310 implies the cluster was found three times in run 1, once in run 2 and not at all in run 3. (9) Whether or not the cluster was deblended (d or blank). (10) Abell identification number: an identification is defined as being an Abell cluster centre within one Abell radius of an EDCC cluster. Where the Abell identification appears in brackets only the clusters' Abell radii overlap.

If the cluster entry has a zero magnitude then it implies that most of its members have been lost to a companion during deblending (so that the background-subtracted magnitude cannot be defined). If $m_{10}=0$ then the richness and background are taken to be zero by default (since the richness cannot be calculated if $\theta_{\rm A}=0$). These clusters are still included since they represent distinct peaks in the original catalogues as determined by the KS test, and also show where the centres are in a blend.

All of the clusters have been checked visually. Where a number is missing from the sequential identification described above, that cluster has been rejected on the basis of this check. Only 'obvious' errors are excluded such as residual diffraction spikes from faint stars, star–star mergers, or nearby, bright face-on spirals, where the nucleus and dense H II regions in the disc are detected as separate objects. As noted above, these objects are listed separately in Table 4. In this table the final column contains our assessment of the actual object detected.

We have also indicated possible errors in our richness and magnitude estimates in Table 3, where the visual inspection gave a clearly different result. These are flagged by a * in the m_{10} (4 clusters) or $n_{\rm clus}$ (82 clusters) columns. A '?' against the cluster identification in general indicates that such clusters could not be distinguished from the surrounding field (43 clusters). It follows that any quoted magnitudes or richness should equally be treated with caution for that cluster. These visual assessments are of course highly subjective and should be used only as a guide and not as absolutes. Most of these possible classification errors are in the richness. Partly, this is due to the greater ease with which such errors can be spotted visually compared to magnitude errors, but it is also in accord with the scatter found previously, whereby the richness values (dependent on m_3) were found to be more uncertain than the m_{10} values. These assessments are also included for those clusters which are deblended; in particular, where a cluster with zero richness and $m_{10}=0$ has a flag against the richness, we assess this as being a good cluster.

The completeness of the catalogue can be estimated in several ways. The number–magnitude relation for the clusters is shown in Fig. 2. The differential and cumulative number counts for those EDCC clusters with more than 30 members and those ACO clusters with the same richness cut-off are shown. The EDCC is partially incomplete at very bright magnitudes (missing three clusters compared to ACO for $b_{\rm j}<17$). Two of these ACO clusters have been deblended in our catalogue and the third lies within a defocused region that was excluded from the EDSGC. Deblending bright large clusters can lead to them being classified wrongly since they overlap with so many other potential centres. The dashed line

Table 2. Error estimates.

Sample	σ_1	σ_3	σ_{m10}	σ_{counts}
All clusters: run 1 v 2	0.54	0.36	0.24	10.4
All clusters: run 1 v 3	0.52	0.31	0.34	9.2
All clusters: run 2 v 3	0.42	0.31	0.26	9.5
$c>30$: run 1 v 2	0.57	0.24	0.15	10.4
$c>30$: run 1 v 3	0.60	0.24	0.19	8.2
$c>30$: run 2 v 3	0.46	0.16	0.15	9.5
Final catalogue	0.34	0.23	0.18	6.9
Final catalogue: $c>30$	0.38	0.15	0.15	6.5
Final catalogue: offset $<2'$	0.32	0.14	0.08	4.6

Table 3. The Edinburgh–Durham Cluster Catalogue.

EDCC	R.A. (h m s)	Dec. (° ′ ″)	m_1	m_3	m_{10}	n_{clus}	n_{back}	θ_A	Field	runs	Deb.	Abell
1	21 26 47.4	−22 29 39.0	17.28	18.13	19.58	21	40	0.151	F531	111	d	2347
2	21 27 17.3	−22 40 41.5	16.88	17.02	18.76	11	19	0.196	F531	010	d	
3	21 28 1.9	−24 1 1.9	15.68	17.62	17.99	40	70	0.269	F531	110	d	
4	21 29 27.7	−24 9 40.9	14.65	17.33	18.12	47*	44	0.255	F531	111	d	
5	21 29 33.9	−22 53 2.0	15.95	17.38	18.56	15	71	0.212	F531	011	d	3778
6	21 29 59.3	−23 1 14.0	15.63	16.78	19.05	8	32	0.178	F531	121	d	
7	21 30 37.5	−23 57 14.8	18.29	18.37	19.04	24*	95	0.179	F531	010	d	
8	21 30 54.0	−26 0 24.8	16.12	18.10	0.00	0	0	0.000	F531	011	d	
9	21 31 31.3	−27 18 28.2	15.24	15.87	17.22	15	7	0.370	F531	110	d	
10	21 31 46.7	−26 15 51.2	15.52	16.22	17.62	22	11	0.313	F531	100	d	
11	21 32 55.6	−26 53 59.2	15.11	16.11	18.17	8	5	0.249	F531	100	d	
12	21 33 55.8	−23 29 41.7	16.42	17.88	18.45	48	67	0.222	F531	011		2357
13	21 36 40.9	−27 19 50.7	17.54	18.27	18.65	38	62	0.205	F531	010		3797
14	21 36 53.1	−26 49 41.3	14.09	17.32	18.15	13	34	0.252	F531	100	d	
15	21 37 31.8	−23 5 51.3	14.41	15.77	17.15	23	10	0.381	F531	113	d	(S 963)
16?	21 37 38.6	−32 37 11.7	17.34	17.39	18.33	33	15	0.233	F466	012	d	(3795)
17?	21 37 56.5	−31 16 30.7	14.55	19.72	20.27	22	16	0.120	F466	001		
18	21 38 6.7	−23 4 21.4	0.00	0.00	0.00	0	0	0.000	F531	001	d	
19?	21 38 11.0	−32 6 50.5	16.00	16.83	18.38	14	9	0.229	F466	100	d	
20	21 38 15.1	−27 0 33.2	17.09	18.14	19.38	28	36	0.161	F531	011	d	
21	21 38 17.2	−29 13 16.2	15.49	16.45	17.90*	7	11	0.279	F466	110		
22?	21 38 22.8	−28 39 24.5	16.95	17.77	18.17	43	52	0.249	F466	011		
23?	21 39 37.7	−31 36 23.8	18.42	18.75	19.84	48	24	0.138	F466	001	d	
24?	21 39 39.8	−31 55 35.3	17.09	18.02	18.33	69	39	0.233	F466	110	d	
25?	21 39 47.0	−32 34 40.3	16.34	17.40	18.36	34	18	0.231	F466	010	d	
26	21 40 35.1	−25 26 13.5	13.67	17.31	18.20	19	40	0.245	F531	100		
27	21 41 0.0	−31 19 51.3	15.86	18.16	18.49	59*	46	0.211	F466	001		
28?	21 41 33.4	−32 28 58.4	17.41	18.03	18.71	48	32	0.200	F466	100	d	
29	21 41 33.5	−24 37 17.4	18.57	19.39	20.12	21	39	0.127	F531	001	d	
31	21 42 27.7	−24 23 33.7	15.89	17.61	18.46	55	45	0.221	F531	011	d	2371
32	21 42 42.3	−27 30 52.0	17.04	19.26	19.69	34*	54	0.145	F531	001		
33	21 42 44.6	−22 42 53.5	16.55	17.31	18.63	15	30	0.207	F531	111		
34	21 42 51.5	−26 10 10.3	17.63	17.77	18.89	50*	38	0.188	F531	011		3805
35	21 43 2.7	−30 9 11.5	15.41	18.02	18.89	34	50	0.188	F466	001	d	
36?	21 43 25.2	−31 7 54.8	17.05	17.50	18.46	19	33	0.221	F466	100	d	
37	21 44 57.1	−30 49 45.3	17.44	17.88	18.13	54*	73	0.254	F466	111	d	
38?	21 45 39.3	−31 58 49.7	17.36	17.87	18.39	40	55	0.228	F466	011		3813
39	21 45 42.2	−28 27 12.9	16.94	17.25	18.34	22	26	0.217	F466	100		
40	21 45 53.1	−27 55 42.8	16.47	16.82	18.65	13	13	0.205	F466	110		
42	21 46 21.9	−30 56 37.8	16.18	17.55	18.21	87	55	0.245	F466	111	d	3814
43	21 46 34.6	−35 54 25.7	16.10	16.73	17.55	30	18	0.323	F404	010	d	
44?	21 46 37.2	−37 36 3.9	16.05	16.36	18.39	6	4	0.228	F404	011	d	
45	21 46 40.2	−34 2 11.8	16.52	16.71	17.78	18	21	0.293	F404	111		(3815)
46	21 46 40.3	−37 6 4.5	16.01	17.06	17.78	57*	17	0.293	F404	111	d	
47?	21 46 45.7	−30 9 10.9	16.65	17.64	18.60	19	40	0.207	F466	100		
48	21 47 32.9	−35 7 5.5	12.70	15.64	17.72	6	4	0.301	F404	220	d	
49?	21 47 34.6	−26 56 12.5	16.57	17.87	18.16	67	75	0.250	F531	110		
50	21 49 2.7	−31 53 30.5	17.39	17.54	18.10	47*	55	0.257	F466	101	d	
51	21 49 22.2	−29 8 1.7	16.35	16.76	17.78	17	30	0.293	F466	111		
52	21 50 12.6	−23 48 46.8	18.60	18.72	19.01	82	71	0.180	F532	011		2385
53	21 50 12.8	−31 47 36.5	17.34	17.83	19.15	16	47	0.172	F466	011	d	
54	21 50 45.7	−42 25 48.9	15.40	16.34	17.87	11	6	0.282	F344	110		(S 978)
55	21 52 4.7	−37 51 18.1	15.88	17.74	17.87	69*	45	0.282	F344	110		
57	21 53 30.9	−30 23 0.4	17.29	18.05	18.19	31	96	0.248	F466	110	d	
58	21 53 38.9	−35 9 38.5	17.25	18.19	18.79	61*	48	0.194	F404	011	d	
59	21 53 42.8	−32 53 38.5	18.29	18.38	19.49	38	44	0.155	F404	001		
60	21 53 47.4	−24 10 5.9	17.04	19.09	19.65	28	57	0.147	F532	001		
61	21 53 59.4	−30 19 37.9	18.24	18.31	0.00	0	0	0.000	F466	001	d	
62	21 54 2.5	−40 10 41.8	15.91	16.08	17.45	16	6	0.336	F344	110	d	
64	21 54 17.0	−38 22 15.8	15.11	16.11	18.09	10*	6	0.257	F344	110		
65	21 54 54.9	−26 57 12.8	17.08	18.58	19.32	53*	56	0.163	F532	001		(3824)
66	21 55 2.0	−39 41 39.2	16.02	16.14	18.02	8	6	0.265	F344	110	d	
67	21 55 35.2	−30 9 33.4	17.58	19.20	19.67	34	60	0.145	F466	001	d	
68	21 55 36.5	−31 7 54.8	16.01	17.08	17.76	34	49	0.296	F466	121		
69	21 55 37.0	−28 49 33.2	13.33	14.54	16.27	8	5	0.594	F466	100		
70	21 56 9.5	−25 26 51.0	16.61	17.51	18.92	12	24	0.186	F532	010		
72	21 56 56.9	−42 20 24.0	16.17	16.84	17.94	47*	24	0.274	F344	110		
73	21 57 16.8	−24 43 45.1	15.53	16.70	18.45	11	12	0.223	F532	100		
75	21 58 7.7	−24 21 16.1	18.45	18.65	18.84	23	79	0.193	F532	010		
76	21 58 41.5	−32 9 44.5	11.92	14.87	17.72	2	1	0.287	F466	100		
77	21 59 10.6	−22 59 33.9	0.00	0.00	0.00	0	0	0.000	F532	021	d	
78	21 59 15.3	−29 56 21.4	18.37	18.49	19.34	18	53	0.164	F466	010		
79	21 59 21.3	−37 46 52.3	15.45	16.65	18.70	4	10	0.200	F404	010		
80	21 59 25.2	−22 48 38.6	14.63	14.79	16.69	10	3	0.461	F532	110	d	S 987
81	21 59 37.5	−30 19 29.4	17.98	18.83	19.53	23	60	0.157	F466	001		
82	21 59 45.7	−41 24 48.0	14.13	16.95	18.05	20*	25	0.262	F344	100		
83	22 0 3.9	−28 37 58.0	16.75	17.33	19.08	7	18	0.170	F466	001		
84	22 0 19.0	−34 47 30.0	17.73	18.21	19.56	21	32	0.144	F404	001		
85	22 2 5.0	−25 29 37.9	17.06	17.67	19.75	6	18	0.143	F532	001		2416
86	22 2 25.6	−30 45 48.0	16.26	17.35	18.73	16	25	0.202	F467	010		3833
87	22 2 41.5	−33 58 25.7	18.74	19.09	19.41	41*	71	0.157	F404	001		
88	22 3 24.2	−39 24 18.7	17.00	17.14	18.31	13	28	0.235	F344	111		S 993
89	22 3 46.7	−36 37 55.4	16.71	17.49	19.42	10	18	0.158	F404	001	d	
90	22 4 9.6	−42 1 18.3	16.25	17.83	18.40	23	52	0.226	F344	110	d	
91	22 4 55.8	−24 39 44.3	17.71	18.56	19.52	29	50	0.153	F532	001		2417
92	22 5 18.0	−41 47 45.2	16.22	17.00	18.26	10	25	0.240	F344	100	d	

Table 3 – *continued*

EDCC	R.A. (h m s)	Dec. (° ′ ″)	m_1	m_3	m_{10}	n_{clus}	n_{back}	θ_A	Field	runs	Deb.	Abell
93	22 5 25.9	−26 44 38.1	17.58	18.49	18.88	35	80	0.189	F532	011		
94	22 5 35.4	−26 22 5.7	17.16	18.51	19.05	50	69	0.178	F532	010		(2418)
95	22 5 39.3	−36 45 45.2	16.35	16.90	18.12	23	28	0.255	F404	110	d	
96	22 6 9.7	−35 21 37.2	14.57	15.11	17.11	9	4	0.387	F404	101		S 997
97	22 6 10.8	−32 19 53.3	17.60	19.11	20.48	10	32	0.112	F467	001		
98	22 6 30.3	−28 43 20.2	17.79	18.17	19.49	19	32	0.145	F467	001		
99	22 6 34.9	−27 33 24.0	14.39	14.99	17.67	4	2	0.307	F532	111		3837
100	22 7 17.3	−28 20 34.5	18.20	18.53	19.19	16	55	0.161	F467	001		3838
101	22 7 33.6	−40 6 23.8	16.28	16.38	18.84	2	6	0.191	F344	010		3840
102	22 7 40.2	−30 27 43.3	16.08	18.79	20.24	18	32	0.122	F467	001		
103	22 8 6.3	−28 42 40.5	19.09	19.40	20.30	20	44	0.120	F467	001		
104	22 8 25.3	−33 15 37.0	17.22	17.32	18.38	25	26	0.219	F404	100		
105	22 8 40.5	−39 2 19.3	17.83	18.50	18.63	45	87	0.206	F344	001	d	3842
106	22 8 53.4	−33 55 34.2	16.32	17.62	18.57	21	36	0.211	F404	100	d	S1000
107	22 9 18.5	−34 19 57.5	14.84	15.82	18.04	2	4	0.263	F404	100	d	
108	22 9 49.0	−38 45 4.7	14.81	16.63	18.72	7	10	0.198	F344	010	d	
110	22 9 55.3	−29 15 23.1	18.02	18.41	19.48	21	45	0.158	F467	001		
111	22 9 58.1	−27 15 51.2	16.03	17.80	18.24	42	64	0.242	F532	110		
112	22 10 10.0	−32 49 10.4	16.67	18.46	19.30	39	46	0.167	F404	001		
113	22 10 51.4	−36 37 9.5	0.00	0.00	0.00	0	0	0.000	F404	100	d	
114	22 11 8.7	−36 54 40.2	15.34	16.82	17.15	57	55	0.381	F404	122	d	S1005
115	22 11 9.1	−35 13 31.2	15.66	17.25	18.58	10	24	0.210	F405	001		(3844)
116	22 11 27.2	−34 42 33.7	16.64	16.97	19.45	4	8	0.148	F404	001		
117	22 12 19.5	−27 21 12.5	16.17	17.09	18.58	12	22	0.212	F533	010		(3846)
118	22 13 18.5	−41 19 4.9	15.34	16.41	18.03	5	12	0.264	F344	010		
119	22 13 21.8	−25 51 52.6	15.77	15.94	18.28	6	6	0.238	F533	111		
120	22 13 35.0	−39 31 55.6	18.20	18.31	18.75	28	67	0.192	F344	001		3853
121	22 13 51.5	−25 24 43.5	16.24	16.53	20.04	2	4	0.136	F533	001		
122	22 14 22.9	−38 36 27.2	17.45	17.69	19.22	18	24	0.161	F344	010		
123	22 14 37.1	−26 31 26.3	16.38	16.96	18.87	8*	18	0.189	F533	011	d	(S1008)
124	22 14 43.9	−35 57 33.1	17.07	18.04	18.46	109	63	0.221	F405	011		3854
125	22 15 6.5	−41 50 55.9	16.15	16.59	18.47	11	11	0.220	F344	100		
126	22 15 8.8	−30 19 50.2	16.18	17.20	18.28	17	28	0.240	F467	100		
127	22 15 41.0	−39 8 55.9	16.38	17.49	18.09	53	52	0.257	F344	111		3856
128	22 15 56.3	−28 34 41.1	16.73	17.95	20.32	2	17	0.120	F467	100		
129	22 16 2.1	−24 26 56.1	14.77	16.34	16.75	36*	31	0.449	F533	111		
130	22 16 6.2	−26 47 19.5	14.42	15.75	17.62	12	7	0.313	F533	111	d	(S1010)
131	22 16 39.2	−34 56 27.0	16.73	17.90	18.18	66	63	0.249	F405	111		3858
132	22 17 5.3	−39 46 11.4	16.06	17.30	18.05	20	40	0.262	F344	100		
133	22 17 37.6	−22 39 45.2	16.52	19.18	20.12	19	39	0.127	F533	001		
134	22 17 40.6	−35 23 52.5	17.67	18.61	19.28	27	50	0.158	F405	001		3866
135	22 18 26.4	−26 17 15.3	15.76	17.87	18.85	16	36	0.180	F533	100		
136	22 18 52.3	−29 3 37.1	16.16	17.60	18.89	40*	25	0.188	F467	011		
137	22 19 17.9	−38 52 56.0	15.80	16.26	19.15	5	4	0.170	F345	101		S1016
139	22 21 21.4	−26 27 16.2	16.70	17.44	18.50	15	31	0.218	F533	011		(S1018)
140	22 21 22.6	−42 3 5.8	16.34	17.33	18.23	10	31	0.243	F345	100		
141	22 22 50.9	−35 11 46.4	16.62	18.77	19.17	38	61	0.175	F405	001		
142	22 23 1.5	−31 21 17.7	14.02	14.84	16.43	10	5	0.526	F467	212	d	
143	22 23 48.5	−42 40 58.4	16.72	18.37	19.42	27	42	0.158	F345	010		
144	22 24 3.2	−32 13 26.3	17.30	18.21	19.08	19	33	0.168	F467	001		3878
145	22 24 56.7	−30 51 11.0	15.07	16.27	16.91	34	27	0.421	F467	111	d	3880
146	22 24 59.8	−24 3 54.5	0.00	0.00	0.00	0	0	0.000	F533	001	d	(2444)
147	22 25 28.0	−24 17 24.5	16.18	17.28	17.69	28	46	0.305	F533	100	d	
148	22 25 39.2	−24 42 57.9	15.89	16.43	18.96	7	10	0.183	F533	001	d	
149?	22 26 24.6	−32 15 32.2	16.88	18.01	18.55	51	41	0.205	F468	010		
150	22 26 28.8	−36 39 4.9	15.67	17.30	19.98	5	10	0.133	F405	001		(3882)
151?	22 27 22.4	−24 10 52.0	17.19	17.28	17.55	12	50	0.323	F533	100	d	
152?	22 27 47.2	−24 34 53.0	17.48	17.64	18.47	5	36	0.220	F533	100	d	
153	22 29 19.8	−31 27 51.9	15.55	16.06	17.30	11	9	0.358	F468	101		
154	22 29 23.4	−39 0 52.5	16.76	18.27	19.78	19	44	0.141	F345	001	d	
155	22 29 26.3	−25 40 49.1	13.28	16.05	16.77	10	20	0.446	F533	111		
156	22 29 53.3	−39 16 50.4	16.88	18.58	19.20	53	76	0.170	F345	001	d	3887
158	22 30 45.3	−36 2 11.7	17.72	19.13	19.29	39*	75	0.166	F405	011		
159	22 31 7.4	−39 19 53.2	19.63	19.63	19.94	22	62	0.134	F345	001	d	
160	22 31 32.4	−37 59 54.1	15.42	16.30	18.00	10	14	0.268	F345	011		3888
161	22 32 54.3	−38 59 17.3	16.23	16.63	17.72	18	26	0.301	F345	011		S1042
162	22 33 4.7	−37 36 45.1	14.87	15.88	18.54	5	5	0.214	F405	010		
163	22 33 6.1	−40 40 55.4	18.09	18.12	18.91	19	56	0.187	F345	010		
164	22 33 17.2	−41 43 42.2	15.86	16.67	17.49	14	28	0.331	F345	100		
165	22 33 35.6	−24 36 25.3	14.88	16.27	17.28	26	18	0.361	F534	111		S1043
166	22 34 4.8	−38 17 43.8	16.56	18.27	18.98	56	77	0.182	F345	011		S1045
168	22 34 22.7	−39 26 53.0	15.80	16.67	19.30	4	15	0.164	F345	011	d	S1047
169	22 34 44.9	−39 45 14.8	17.31	17.53	17.98	19	68	0.270	F345	110	d	
170	22 35 9.7	−30 56 26.5	15.98	17.43	18.48	15	23	0.219	F468	001		3892
171	22 35 11.0	−24 9 40.5	17.74	18.01	18.92	26	37	0.189	F534	001		3893
172	22 35 50.4	−37 9 50.4	14.80	15.65	17.05	21	15	0.397	F405	122	d	3895
173	22 35 57.3	−36 39 56.2	16.23	16.52	17.78	18	43	0.293	F406	022	d	
174?	22 36 17.9	−22 48 45.5	15.92	16.34	18.09	14	10	0.258	F534	121		
175	22 36 27.4	−38 5 29.3	16.21	17.53	18.40	42	59	0.227	F345	112		S1051
176	22 36 54.3	−36 26 25.4	0.00	0.00	0.00	0	0	0.000	F406	110	d	(S1050)
177	22 37 27.4	−24 8 2.7	17.87	18.82	19.42	31*	54	0.163	F534	001		3900
178	22 37 50.6	−34 14 33.4	16.42	17.67	18.22	35*	43	0.241	F406	010		
179	22 38 58.7	−36 33 51.5	16.04	19.29	20.29	8	39	0.119	F406	001		
180?	22 39 7.7	−29 27 43.4	16.16	16.74	17.54	21	21	0.327	F468	100		
181	22 39 29.2	−38 51 44.5	18.95	19.32	19.44	95	78	0.156	F345	001		
182	22 39 42.1	−25 15 16.3	15.75	16.44	18.06	12	9	0.261	F534	111		

Table 3 – *continued*

EDCC	R.A. (h m s)	Dec. (° ′ ″)	m_1	m_3	m_{10}	n_{clus}	n_{back}	θ_A	Field	runs	Deb.	Abell
183	22 40 6.8	−38 20 35.0	18.62	18.73	19.31	35	82	0.166	F345	001		
184	22 40 33.3	−23 43 11.2	16.15	16.86	19.00	5	8	0.181	F534	100		
185	22 41 14.0	−40 7 40.6	13.35	15.90	17.23	15	16	0.376	F345	100		S1055
186	22 42 28.1	−38 4 2.0	17.32	17.86	18.87	14	51	0.187	F345	100		S1056
187	22 43 23.9	−34 15 32.2	16.36	16.74	17.71	16	26	0.302	F406	100	d	
188	22 43 39.4	−36 21 46.7	15.20	16.29	17.50	29	23	0.329	F406	112		3912
189	22 44 0.9	−39 29 1.8	16.74	16.91	19.70	3	10	0.144	F346	001		
190	22 44 30.4	−41 9 45.4	16.45	17.01	18.41	17	24	0.226	F346	010	d	
191	22 44 41.1	−34 35 46.6	16.95	17.33	19.31	9	21	0.164	F406	001	d	
192?	22 45 18.6	−31 29 26.7	17.67	18.03	18.52	18	48	0.216	F468	010	d	
194	22 45 44.1	−28 51 51.6	16.78	17.58	19.11	23*	18	0.175	F468	011		3918
195	22 46 14.1	−28 21 50.2	15.87	16.92	18.71	10	10	0.200	F468	001		
196	22 46 15.2	−33 5 43.8	16.12	16.50	18.54	7	9	0.214	F406	001	d	S1064
197	22 46 16.1	−37 41 58.6	13.66	15.82	16.70	19	23	0.459	F406	100		S1065
198	22 46 29.7	−41 10 2.1	18.17	18.60	18.76	61	86	0.196	F346	010	d	3920
199	22 46 39.9	−38 55 49.0	16.44	18.98	19.69	12	62	0.147	F346	001		
200	22 46 42.4	−23 47 57.0	17.38	18.90	19.18	62	56	0.171	F534	011		2488
201	22 47 13.5	−31 26 25.6	17.15	17.71	18.10	46*	50	0.257	F468	111	d	
202	22 48 2.1	−33 3 2.8	16.52	16.61	17.81	22	20	0.289	F406	100	d	
203	22 48 13.2	−26 20 35.4	17.81	18.04	18.37	31*	44	0.230	F534	111		2493
204	22 48 32.8	−35 18 5.4	17.08	17.32	18.19	23	32	0.231	F406	100		
205	22 48 43.9	−34 35 42.0	14.98	17.14	18.50	15	22	0.217	F406	100		
206	22 48 59.1	−33 40 16.2	16.72	18.57	19.47	58	52	0.156	F406	001	d	3926
207	22 49 13.2	−32 28 0.5	15.68	17.39	18.95	13	19	0.186	F469	010		3929
208	22 49 18.6	−39 31 20.0	17.51	19.56	19.92	16	51	0.141	F346	001		
209	22 49 31.7	−33 49 22.9	17.00	18.98	19.47	34	64	0.156	F406	011	d	3928
210	22 49 56.5	−31 24 10.6	16.37	17.28	19.51	7	10	0.152	F469	100		3930
211	22 50 0.9	−26 17 17.0	17.58	18.96	19.17	81*	56	0.171	F534	011		2499
212	22 50 7.4	−23 15 45.8	17.86	19.19	19.78	30*	49	0.143	F534	001		
213	22 50 29.0	−28 37 38.0	17.31	17.76	19.87	8	13	0.137	F469	001		
214	22 50 35.9	−35 35 1.6	16.91	18.93	19.43	31	59	0.158	F406	001		
215	22 50 38.9	−29 48 46.9	16.39	16.83	18.49	8	12	0.219	F469	100		
216	22 50 40.5	−25 47 13.6	16.86	17.39	17.98*	79	34	0.270	F534	111		2500
217	22 50 42.2	−30 24 50.8	16.78	16.90	17.82	25*	21	0.275	F469	100		
218	22 50 42.7	−29 8 36.1	16.55	16.94	18.69	10	11	0.201	F469	011		
219	22 51 12.1	−37 17 9.6	15.71	16.97	19.40	2	12	0.166	F406	001		
220	22 51 39.3	−24 45 2.8	16.26	18.70	19.54	17	38	0.149	F534	001		
221	22 52 19.9	−38 55 31.1	17.95	18.41	19.95	19	35	0.133	F346	001		
222	22 52 43.4	−34 10 54.4	14.09	15.66	17.40	10	8	0.343	F406	100		(3934)
223	22 52 52.9	−42 29 40.8	15.22	16.12	18.27	7	7	0.239	F346	110		
224	22 53 22.5	−38 2 44.4	16.29	17.32	18.48	15	33	0.219	F346	100		
225	22 53 30.8	−28 41 33.3	16.97	17.54	18.78	20	20	0.186	F469	001		3943
226?	22 54 14.2	−27 8 41.1	15.19	16.24	17.67	25	9	0.307	F534	111		(3948)
227	22 55 4.7	−39 21 54.3	16.68	17.67	19.52	10	24	0.151	F346	001		3945
228	22 55 38.9	−31 5 19.5	0.00	0.00	0.00	0	0	0.000	F469	110	d	(S1075)
229	22 56 2.3	−30 58 13.7	14.36	16.62	17.37	39	24	0.348	F469	111	d	
230	22 56 32.8	−31 7 11.7	0.00	0.00	0.00	0	0	0.000	F469	001	d	
231	22 58 5.1	−24 26 44.0	16.50	17.67	18.65	21	28	0.204	F535	011		2518
232	22 58 14.0	−26 33 2.2	18.69	18.78	18.95	10	62	0.178	F535	010		
234	22 59 37.6	−29 28 18.4	18.03	18.46	19.25	26*	43	0.172	F469	001		3958
235	22 59 55.3	−33 38 6.3	17.00	17.75	19.05	18	28	0.178	F407	001	d	3959
236?	23 0 5.0	−28 45 55.9	17.14	17.69	19.15	20	20	0.179	F469	010		
237	23 0 5.6	−35 12 12.7	16.55	18.78	19.38	30	57	0.161	F407	001		3960
239	23 0 50.6	−33 54 25.3	16.90	17.52	19.36	10	18	0.162	F407	100	d	
240	23 0 50.6	−42 35 23.4	16.95	17.38	18.64	18	29	0.206	F346	010		S1084
241	23 1 16.8	−32 6 31.0	16.25	17.21	17.95	26	34	0.273	F469	111	d	
242	23 1 42.5	−24 23 10.1	17.82	19.20	19.49	73*	68	0.155	F535	001		2526
243	23 2 14.2	−32 53 35.4	16.55	16.60	18.10	20	15	0.257	F469	111	d	S1086
244	23 2 36.8	−25 37 21.1	18.06	20.05	20.22	34	33	0.122	F535	001		2527
245	23 2 49.9	−32 28 18.2	15.74	16.55	18.56	8	9	0.212	F469	100	d	
246	23 2 53.2	−33 5 22.7	19.31	0.00	0.00	0	0	0.000	F407	001	d	
247	23 2 56.1	−39 22 14.5	16.49	17.92	18.35	57	65	0.232	F346	011		3968
248	23 2 59.6	−30 55 33.7	14.60	15.62	17.47	11	6	0.333	F469	111		
249	23 3 0.8	−29 21 39.5	16.58	18.94	0.00	0	0	0.000	F469	100	d	
250	23 3 8.6	−34 43 53.0	16.12	18.89	19.74	34	42	0.136	F407	001		
251	23 3 11.0	−35 45 39.8	17.13	18.34	19.67	18	34	0.149	F407	001		
252	23 3 59.1	−29 12 58.9	16.34	17.55	18.31	45	32	0.236	F469	001	d	
253	23 5 1.3	−22 52 46.4	17.69	18.31	18.69	73*	67	0.201	F535	002		2534
254	23 5 26.3	−42 32 39.0	16.45	16.79	17.78	4	34	0.313	F346	100		
255	23 6 0.0	−33 9 58.9	16.41	16.78	19.30	3	6	0.163	F407	001		
256	23 7 36.2	−23 12 39.6	16.93	17.86	18.48	51*	49	0.219	F535	011	d	2541
257	23 7 59.8	−34 22 27.4	16.64	17.10	18.86	11	13	0.190	F407	011		
258	23 8 1.3	−22 55 14.8	16.41	17.98	18.73	41	45	0.198	F535	011	d	2546
259	23 8 14.0	−40 45 16.4	16.54	18.68	19.27	38	63	0.166	F346	010	d	(3977)
260	23 8 28.2	−28 59 43.2	11.84	16.39	17.88	20	11	0.281	F469	121	d	3978
261	23 9 9.4	−29 19 41.1	16.75	17.37	18.33	26	30	0.233	F469	111	d	S1096
262	23 9 17.9	−41 49 42.4	16.97	17.76	19.09	16	31	0.169	F346	010		
263	23 9 30.4	−41 2 39.1	16.58	17.21	18.67	20	27	0.203	F346	010	d	
264	23 9 38.0	−25 14 56.3	17.52	18.82	19.08	56	71	0.176	F535	011		2553
265	23 9 58.0	−39 25 31.7	16.63	18.69	19.28	39	63	0.166	F347	001		
266	23 10 19.5	−28 38 54.9	12.37	16.74	19.09	5*	5	0.176	F470	011		3980
267	23 10 24.1	−30 36 29.3	16.80	17.48	18.57	29*	25	0.211	F469	110		
268?	23 11 35.8	−26 46 7.1	17.73	19.01	19.65	44	54	0.147	F535	001		
269	23 12 32.5	−38 2 9.0	14.58	17.64	18.54	54	34	0.214	F347	011		3984
270	23 13 24.3	−23 39 58.8	16.67	17.48	18.27	21	37	0.239	F535	101		3985
271	23 13 28.7	−38 38 39.0	17.32	18.72	19.79	26	48	0.148	F347	001		

Table 3 – *continued*

EDCC	R.A. (h m s)	Dec. (° ′ ″)	m_1	m_3	m_{10}	n_{clus}	n_{back}	θ_A	Field	runs	Deb.	Abell
272	23 13 35.3	−39 12 1.8	15.99	16.26	18.80	2	5	0.193	F347	010	d	
273	23 14 23.0	−39 34 32.7	17.16	17.41	18.42	25	30	0.225	F347	101	d	
274	23 14 47.5	−37 28 32.7	18.53	18.74	19.74	19	38	0.134	F407	001		
275	23 14 52.5	−25 37 9.1	16.25	17.72	19.11	8	22	0.171	F535.	001		
276	23 15 25.8	−35 54 41.1	18.46	18.75	19.50	50	46	0.155	F407	001		3989
277	23 15 34.9	−36 34 4.8	16.64	18.38	19.39	33	39	0.161	F407	001		S1109
278	23 15 40.9	−33 56 47.9	17.32	17.40	19.26	8	13	0.167	F407	001		
279	23 15 47.7	−27 47 16.6	16.23	17.53	18.34	37	30	0.232	F535	110		
281	23 16 23.3	−34 35 3.4	16.47	17.25	18.20	11	25	0.246	F407	100		
282	23 16 30.9	−37 43 57.9	18.71	19.62	20.03	24	44	0.134	F407	001		
283	23 16 37.6	−42 18 28.7	11.23	12.30	16.38	1*	0	0.548	F347	110	d	S1111
284	23 17 3.3	−22 44 31.0	17.98	18.38	19.45	31	50	0.167	F536	001		2576
285	23 18 12.7	−42 9 24.7	0.00	0.00	0.00	0	0	0.000	F347	110	d	(3998)
286	23 18 19.4	−29 8 48.3	16.47	17.49	20.06	6	8	0.128	F470	001		
287	23 18 39.1	−23 25 49.0	15.71	16.78	18.37	20	14	0.230	F536	112		2580
288	23 19 39.4	−40 57 9.3	16.48	16.64	18.73	8	10	0.209	F347	100		4000
289	23 20 16.0	−26 33 20.8	17.55	18.54	19.55	40	42	0.157	F536	001		2585
290	23 20 23.5	−31 41 47.7	15.99	18.33	19.00	29	45	0.176	F470	010		
291	23 21 30.0	−22 50 16.3	17.31	18.78	19.24	20	68	0.167	F536	010		(2587)
292	23 22 19.4	−30 35 45.6	16.45	17.07	18.32	14	17	0.235	F470	100	d	(S1119)
293	23 22 26.0	−23 41 59.2	14.79	17.59	18.24	27	45	0.242	F536	111		2596
294?	23 22 49.0	−29 47 51.8	15.76	17.92	18.16	27	53	0.249	F470	100		
295	23 23 30.3	−39 30 39.0	15.13	16.03	17.59	16	9	0.317	F347	110		
296	23 23 33.9	−30 49 59.8	15.98	16.75	0.00	0	0	0.000	F470	100	d	
297	23 23 46.2	−24 14 59.1	16.86	17.41	18.04	60*	38	0.263	F536	122		2599
298	23 24 5.9	−22 42 22.6	17.82	17.90	18.35	25	63	0.232	F536	111		2600
299	23 24 10.1	−32 0 0.0	17.51	18.79	19.63	43	45	0.143	F470	001		S1123
300?	23 25 32.8	−25 10 58.2	17.96	18.13	18.73	17	48	0.198	F536	010		
301	23 25 39.6	−29 25 39.6	16.80	17.07	18.89	16	10	0.188	F470	011		S1127
302	23 25 42.1	−36 41 48.4	16.17	18.07	18.54	21	60	0.227	F408	010		
303	23 26 20.5	−23 39 26.9	16.63	17.03	18.38	12	19	0.229	F536	111		2605
304	23 26 43.1	−30 25 58.3	17.24	18.26	19.48	9	33	0.158	F470	001		
305	23 26 53.8	−31 22 14.1	15.46	16.02	18.45	6	3	0.221	F470	100		S1129
306	23 27 9.6	−36 2 34.8	16.33	17.28	17.88	21	41	0.286	F408	100		
307	23 27 31.1	−39 33 24.8	14.88	16.16	17.72	11	10	0.301	F347	111		4008
308	23 27 42.9	−35 13 24.0	15.26	15.93	17.09	26	12	0.391	F408	111	d	
309	23 27 57.2	−26 24 5.1	16.57	17.34	19.56	5	9	0.153	F536	001		2609
310	23 27 59.1	−29 31 52.8	16.49	17.92	18.69	38	32	0.201	F470	011		4009
311	23 28 36.0	−36 47 41.4	14.66	0.00	0.00	0	0	0.000	F408	011	d	(4010)
312	23 29 13.0	−34 22 0.5	16.64	17.13	17.85	24	33	0.285	F408	110	d	(4012)
313	23 29 18.9	−30 21 8.1	16.33	16.70	18.36	16	10	0.231	F470	110		
314	23 29 19.2	−34 41 12.1	16.86	17.53	19.13	17	33	0.174	F408	001	d	4011
315	23 29 20.2	−35 34 4.3	17.54	17.96	19.83	9	30	0.138	F408	001	d	4013
316	23 29 49.8	−36 31 28.1	15.92	16.51	17.03	96*	33	0.400	F408	110	d	
317	23 31 19.4	−33 55 41.1	17.29	18.69	19.20	26	64	0.172	F408	010		
318	23 31 52.7	−32 35 44.7	15.37	17.28	18.10	25	32	0.257	F470	010	d	
319	23 33 8.4	−38 47 46.7	16.45	17.26	18.29	7	26	0.237	F347	100		
320	23 33 26.2	−31 52 26.5	14.64	16.51	17.83	20	13	0.287	F470	111		S1136
321	23 33 30.3	−32 47 38.9	15.35	16.31	18.30	8	7	0.237	F408	111	d	
322	23 33 36.9	−36 12 10.9	16.47	17.13	18.58	27	20	0.210	F408	012		
323	23 33 51.4	−30 39 58.7	16.42	16.86	18.66	10	10	0.204	F470	011		
324	23 34 3.4	−24 29 17.2	18.20	18.22	19.00	33	41	0.181	F536	011		2628
325	23 34 52.0	−31 17 6.3	16.38	17.59	18.09	0	44	0.265	F471	100		
326	23 35 9.7	−38 29 18.9	15.64	16.82	18.46	17	13	0.221	F347	110		4021
327	23 35 26.5	−40 57 38.8	15.21	16.36	18.14	13	8	0.253	F347	110		
328	23 35 35.1	−31 47 24.6	16.23	17.65	19.48	13	16	0.156	F471	100		
329	23 38 11.4	−30 34 11.6	16.49	17.17	18.46	10	17	0.221	F471	100	d	S1142
330	23 38 12.9	−37 50 24.9	17.15	18.28	20.00	13	59	0.131	F348	010	d	4026
331	23 38 15.2	−25 8 28.6	17.10	19.44	19.62	78	60	0.148	F536	001		2641
332	23 39 4.3	−29 28 46.3	15.06	17.08	17.73	50*	31	0.299	F471	110		
333	23 39 8.4	−37 47 31.5	16.53	18.32	19.78	18	58	0.141	F348	011	d	
334	23 39 31.2	−42 21 48.6	16.32	17.52	18.53	17	23	0.224	F348	100		
335	23 39 36.3	−30 28 45.3	16.23	18.16	18.83	17	44	0.192	F471	111	d	
336	23 40 40.0	−36 31 17.6	14.79	15.36	16.48	12	14	0.504	F408	100		
338	23 41 5.9	−38 32 21.0	15.57	17.31	19.10	8	15	0.175	F348	001		4029
339	23 41 27.7	−34 46 32.7	15.65	17.43	17.94	20	43	0.256	F408	100		
341	23 42 20.2	−24 3 39.5	15.35	15.66	17.32	9	6	0.355	F537	101		
342	23 42 29.3	−26 17 35.6	16.75	17.02	17.68	19	26	0.306	F537	100	d	2660
343	23 42 33.3	−42 1 15.2	17.73	17.81	18.69	13	26	0.207	F348	010		
344	23 42 45.5	−24 45 52.8	16.43	18.84	19.84	26	40	0.136	F537	001		4031
345	23 43 34.3	−23 27 36.6	15.62	16.91	18.05	13	17	0.262	F537	110		S1146
346	23 43 45.3	−28 35 50.7	0.00	0.00	0.00	0	0	0.000	F471	001	d	
347	23 44 31.9	−33 53 46.3	17.71	18.63	19.38	38	50	0.156	F408	001		4035
348	23 44 33.7	−28 31 40.6	13.77	15.20	15.90	43*	24	0.783	F471	121	d	4037
349	23 45 9.8	−38 46 58.1	14.71	15.21	16.97	11	6	0.394	F348	100		
350	23 45 40.7	−36 32 37.9	19.54	19.72	19.91	54	47	0.138	F408	001		4039
351	23 46 21.8	−31 34 17.7	18.78	18.96	19.78	33	41	0.141	F471	001		4043
352	23 46 34.3	−35 15 21.6	16.06	16.59	18.06	19	15	0.249	F408	100		
353	23 46 51.1	−27 14 37.4	16.07	18.33	19.10	50	42	0.176	F537	011		4044
354	23 47 8.8	−29 23 54.1	15.01	15.64	17.38	10	7	0.346	F471	100	d	S1155
355	23 47 18.1	−25 0 13.5	18.65	18.87	19.39	40	56	0.158	F537	001		2663
356	23 47 21.2	−35 59 3.5	15.40	16.52	18.86	5	8	0.190	F408	001		
357?	23 47 51.2	−37 27 13.3	19.21	19.43	19.75	43	58	0.143	F348	001		
358	23 48 11.4	−39 5 2.6	15.22	17.55	18.41	11	28	0.209	F348	100		
359	23 48 26.6	−38 43 20.8	18.30	19.26	19.56	66	63	0.149	F348	001		4048
360	23 48 26.6	−34 41 56.4	16.16	0.00	0.00	0*	0	0.000	F349	100	d	

Table 3 – *continued*

EDCC	R.A. (h m s)	Dec. (° ′ ″)	m_1	m_3	m_{10}	n_{clus}	n_{back}	θ_A	Field	runs	Deb.	Abell
361	23 49 2.4	−28 37 44.0	14.17	15.34	17.04	17*	12	0.399	F471	100	d	4049
362	23 49 58.5	−34 40 29.5	15.09	16.53	17.32	36*	31	0.355	F349	112	d	S1157
363	23 50 7.6	−34 25 12.5	14.89	0.00	0.00	0	0	0.000	F349	001	d	
365	23 51 56.5	−32 51 53.5	16.96	17.91	19.51	1	24	0.153	F349	100		
366	23 52 19.6	−27 56 40.0	15.60	16.89	17.78	32	26	0.293	F471	111		4053
367	23 52 40.8	−28 49 9.8	17.16	18.70	18.87	54	69	0.190	F471	001		4054
368	23 53 0.7	−33 56 6.4	16.46	17.66	18.59	26	45	0.225	F349	010		S1161
369	23 53 28.3	−37 33 48.6	18.59	18.70	19.61	24	56	0.153	F348	001		4056
370	23 53 49.7	−31 38 26.1	14.62	16.59	17.56	9	20	0.321	F471	100		
371	23 54 4.4	−36 55 14.2	16.62	18.81	19.68	49	55	0.145	F349	010		4058
372	23 54 18.2	−34 54 40.8	13.86	14.89	16.48	14	7	0.508	F349	111	d	4059
373	23 54 37.1	−32 53 39.6	10.09	16.61	17.62	21	22	0.313	F349	111		
374	23 54 57.4	−37 53 8.8	16.44	16.76	18.64	9	10	0.206	F348	011		S1164
375	23 55 50.9	−24 41 34.5	18.49	18.64	19.30	41	46	0.164	F537	001		2685
376	23 56 5.6	−34 36 9.8	15.74	0.00	0.00	0	0	0.000	F349	122	d	
377	23 56 26.4	−32 9 31.6	15.17	17.26	17.48	60	61	0.332	F471	100	d	
378	23 56 45.7	−32 10 44.0	17.57	0.00	0.00	0	0	0.000	F471	011	d	
380?	23 56 54.5	−31 37 42.1	16.44	16.92	18.34	21	17	0.232	F471	111	d	
381	23 57 14.2	−39 45 34.2	16.71	18.00	18.50	64	47	0.218	F348	110		4068
382	23 57 37.7	−25 29 52.7	16.81	17.19	18.51	20	15	0.217	F537	111		2690
383	23 57 47.9	−30 39 55.6	16.74	19.31	19.61	46*	57	0.145	F409	001		4070
384?	23 58 14.3	−28 54 56.6	17.60	18.53	19.23	26	43	0.164	F409	010		
385	23 58 25.9	−37 5 11.1	18.90	18.94	19.64	24	57	0.149	F349	001		S1170
386	23 58 28.3	−38 56 36.9	15.30	17.83	18.47	24	42	0.220	F348	100		S1172
387	23 58 35.2	−36 39 0.0	15.80	17.63	18.55	35	43	0.213	F349	111	d	4074
388	23 58 53.9	−27 54 6.8	14.22	15.38	16.79	11	8	0.442	F409	110	d	S1171
389	23 58 56.2	−39 26 25.4	16.55	17.69	18.42	13	36	0.222	F348	100		
390	23 59 26.2	−25 23 58.5	16.05	17.55	19.15	12	16	0.171	F537	001		
391	23 59 43.6	−32 3 49.1	16.77	18.52	19.92	18	32	0.134	F409	001		
392	0 0 13.9	−34 56 38.4	17.65	17.73	18.33	42	60	0.233	F349	111		2715
393	0 0 30.3	−30 12 46.7	15.98	16.36	18.06	10	11	0.261	F409	110		S 2
394	0 0 32.1	−36 12 58.9	14.57	16.71	17.22	29	44	0.370	F349	111	d	2717
395	0 0 33.8	−28 10 9.8	15.77	17.45	0.00	0	0	0.000	F409	100	d	(S 3)
396	0 0 37.9	−27 28 15.6	15.97	17.44	18.64	16	31	0.206	F472	111	d	2716
397	0 1 0.8	−42 12 53.2	16.61	18.38	19.03	31	43	0.175	F293	010		2718
398	0 1 25.3	−23 25 15.7	17.09	18.13	18.76	34	42	0.196	F472	101		2719
399?	0 1 56.3	−42 35 23.9	16.89	18.66	19.14	36	60	0.181	F293	010		
400	0 3 39.1	−34 58 49.1	16.30	17.64	18.28	98	51	0.238	F349	111	d	2721
401	0 3 41.5	−39 1 25.8	18.80	19.34	20.09	34	43	0.127	F293	001		
402	0 3 53.0	−26 36 36.5	17.08	17.41	18.07	25	39	0.279	F472	100		
403	0 4 50.4	−34 57 44.5	18.42	18.51	18.98	40	90	0.182	F349	001	d	
404	0 5 17.7	−25 25 33.0	16.68	17.67	18.34	9	36	0.232	F472	100		
405	0 6 33.3	−42 4 13.9	17.33	18.09	18.52	16	51	0.210	F293	010		
406	0 6 34.0	−25 55 41.6	18.35	18.52	19.28	23	44	0.166	F472	001		
407	0 6 38.9	−35 35 0.2	15.08	16.53	17.78	16	17	0.293	F349	110	d	S 12
408	0 7 27.8	−35 56 8.6	16.85	18.13	18.45	52	78	0.222	F349	111	d	2730
409	0 8 41.1	−30 14 41.7	15.43	16.57	17.80	8	16	0.287	F409	100		
410	0 8 46.0	−29 7 35.1	15.03	16.15	17.44	25	12	0.337	F409	111		2734
411	0 10 23.1	−42 28 55.6	16.40	17.06	18.44	16	21	0.232	F293	010		2736
412	0 10 39.3	−35 46 6.4	15.87	16.40	17.42	24	18	0.340	F349	111		
413	0 10 54.4	−24 30 43.9	14.19	17.86	18.45	11*	63	0.222	F473	111	d	
414	0 11 11.7	−38 1 36.9	16.54	17.57	18.92	18	22	0.186	F294	001	d	S 17
415?	0 11 18.3	−37 35 50.0	15.29	17.36	17.74	42	44	0.298	F293	111	d	
416	0 11 23.6	−36 32 37.2	16.54	17.31	18.25	4	36	0.241	F349	111		
417	0 11 58.0	−24 30 44.7	0.00	0.00	0.00	0	0	0.000	F473	001	d	
418	0 12 30.2	−24 9 58.6	15.12	15.72	16.59	31	11	0.481	F473	121	d	0014
419	0 12 49.7	−26 21 9.9	17.05	18.12	18.75	48	41	0.197	F473	011		15
420	0 13 29.5	−37 25 8.2	18.38	18.65	19.03	71	65	0.179	F350	011		2750
421	0 13 35.9	−35 13 53.1	16.38	18.04	18.70	55	55	0.200	F350	001	d	2749
422	0 13 44.9	−39 44 10.1	15.79	16.68	18.39	13	9	0.213	F294	100		
423	0 13 56.0	−31 32 46.7	17.21	18.52	19.99	21*	62	0.131	F410	001	d	2751
424	0 14 5.9	−34 7 59.0	17.64	17.92	18.16	24	75	0.254	F350	010		
425	0 14 46.6	−26 55 8.2	16.14	18.33	18.82	45	43	0.186	F473	010		
426	0 14 56.2	−31 42 27.7	17.76	17.88	18.69	44	36	0.201	F410	010	d	
427	0 14 57.7	−24 28 49.9	15.17	16.64	18.07	14	14	0.260	F473	111	d	
428	0 15 9.5	−27 37 24.2	17.63	18.27	19.23	24	33	0.168	F473	001		
429	0 15 23.2	−35 25 2.5	16.81	17.52	17.91	109	55	0.277	F350	111	d	2755
430	0 16 6.0	−28 12 51.6	17.11	17.99	18.53	23	40	0.215	F410	111		
431	0 16 17.4	−42 1 24.3	16.35	16.66	18.14	24	15	0.253	F294	020	d	2758
432	0 16 20.1	−30 56 8.7	16.54	17.03	18.19	16	19	0.249	F410	100		2759
433	0 16 55.3	−25 55 1.4	0.00	0.00	0.00	0	0	0.000	F473	001	d	
434	0 17 29.9	−42 14 16.7	16.28	17.77	18.40	31	58	0.227	F294	010	d	2763
435	0 17 49.1	−40 43 41.9	17.69	17.88	18.96	14	31	0.183	F294	010		
436	0 18 0.9	−34 12 28.4	16.98	17.87	18.86	30	40	0.189	F350	011		
437	0 18 1.2	−25 54 26.3	17.50	17.83	17.97	124	59	0.271	F473	111	d	22
438	0 20 23.5	−38 24 12.6	17.12	17.56	18.63	33	26	0.207	F294	011		2767
439	0 21 48.8	−34 16 19.5	18.32	18.81	18.95	53*	71	0.178	F350	010		
440	0 21 50.3	−40 23 53.4	15.14	16.27	17.85	10	10	0.285	F294	010		2771
441	0 22 37.8	−38 16 5.7	18.14	18.15	18.59	40	51	0.209	F294	011		2772
442	0 22 52.2	−33 22 0.0	14.52	15.81	17.18	16	10	0.375	F350	110	d	
443	0 23 4.7	−33 17 38.6	15.60	17.36	0.00	0	0	0.000	F350	001	d	(S 41)
444	0 25 12.6	−36 59 48.2	16.01	17.88	18.59	23	35	0.209	F350	010		S 51
445	0 25 40.8	−27 51 7.2	16.37	17.23	18.18	4	21	0.236	F473	100		
446	0 25 44.0	−35 43 4.5	16.51	17.27	18.72	23	15	0.198	F350	011		
447	0 26 7.8	−23 54 4.3	16.67	17.80	18.26	77	48	0.241	F473	111		42
448	0 26 34.0	−30 26 26.8	16.84	17.56	18.19	51	35	0.248	F410	122		2778

Table 3 – *continued*

EDCC	R.A. (h m s)	Dec. (° ′ ″)	m_1	m_3	m_{10}	n_{clus}	n_{back}	θ_A	Field	runs	Deb.	Abell
449	0 26 35.8	−35 16 59.3	17.41	17.71	18.72	33	26	0.198	F350	111		
450?	0 27 23.4	−29 45 1.3	15.02	17.34	17.78	45	40	0.293	F410	110		2780
451	0 28 4.2	−24 27 29.3	19.12	19.18	19.61	34	61	0.156	F473	001		47
452	0 28 50.0	−23 1 32.4	14.67	15.48	18.63	2	2	0.207	F473	101		
453	0 29 11.5	−23 55 1.5	17.43	17.70	19.32	14	20	0.163	F473	011		0051
454	0 31 32.6	−34 32 46.7	15.14	18.56	20.01	23	23	0.124	F350	001		
455	0 32 52.2	−32 39 1.7	19.04	19.21	19.88	31	43	0.141	F350	001		
456	0 33 25.2	−24 4 3.4	16.65	17.54	18.00	33	45	0.268	F474	100		
457	0 33 35.7	−26 22 7.2	15.41	16.31	17.95	11	10	0.273	F474	111		
458	0 33 44.6	−28 32 56.5	0.00	0.00	0.00	0	0	0.000	F411	001	d	
459	0 34 7.1	−28 37 8.4	14.15	16.20	18.54	4	10	0.214	F411	010	d	
460	0 34 47.1	−28 44 47.4	16.94	17.83	18.53	27	70	0.215	F411	111	d	2798
461	0 35 10.7	−31 5 28.7	16.13	16.44	18.60	7	6	0.208	F411	111		(2794)
462	0 35 14.5	−39 23 42.4	15.82	16.81	17.37	45	26	0.348	F294	211		2799
463	0 35 28.5	−25 27 55.6	16.12	16.76	17.48	21	30	0.332	F474	110	d	2800
464	0 35 58.5	−29 19 51.5	15.37	16.59	18.57	8	11	0.211	F411	111	d	2801
465	0 36 21.3	−27 29 10.5	14.75	16.71	19.18	6	7	0.171	F474	010		
466	0 36 24.1	−31 53 26.9	16.82	18.72	19.27	50	46	0.171	F411	001		2802
468	0 36 46.3	−24 16 44.1	15.96	17.29	17.87	18	36	0.283	F474	110		(0080)
469	0 37 13.0	−29 10 20.8	14.34	16.79	18.24	17	16	0.242	F411	111	d	2804
470	0 37 26.4	−26 26 25.1	16.88	17.95	18.79	38	34	0.194	F474	011		
471	0 37 43.3	−24 56 48.3	16.67	16.76	17.51	36	27	0.328	F474	111		80
472	0 37 57.2	−31 49 9.2	17.23	17.83	19.86	7	13	0.137	F411	001		
473	0 40 3.7	−28 50 23.2	16.10	17.11	17.92	67	31	0.277	F411	121		2811
474	0 40 44.7	−26 19 53.9	16.84	17.03	17.54	44	36	0.324	F474	121		0088
475	0 41 6.0	−22 34 15.0	14.44	16.61	18.10	12	12	0.255	F474	100		
476	0 41 35.6	−25 41 28.9	17.11	17.88	18.49	8	40	0.219	F474	100		
477	0 43 14.9	−23 27 16.3	18.08	18.27	19.02	43	41	0.190	F474	001		0097
479	0 45 54.9	−38 45 19.6	16.83	17.91	19.47	16	19	0.149	F295	001		2822
480	0 45 56.6	−42 17 20.8	16.00	16.33	18.11	10	7	0.256	F295	110	d	
481	0 46 29.9	−34 29 4.6	16.06	16.33	17.28	14	14	0.360	F351	110		S 83
482	0 46 50.3	−29 47 22.0	17.15	17.68	18.06	61	54	0.261	F411	111		S 84
483	0 47 38.0	−42 10 1.3	17.03	17.58	0.00	0	0	0.000	F295	100	d	
484	0 48 20.4	−42 27 43.6	15.53	16.51	0.00	0	0	0.000	F295	100	d	
485	0 48 56.3	−28 46 50.4	16.44	16.70	17.63	19	24	0.312	F411	111		2829
486	0 49 7.9	−42 30 7.6	17.51	17.93	0.00	0	0	0.000	F295	010	d	
487	0 49 37.0	−34 14 31.0	16.86	17.41	18.25	23	28	0.243	F351	100		S 88
488	0 50 1.9	−35 16 59.5	14.90	17.00	17.60*	7*	42	0.315	F351	011	d	
489?	0 51 1.7	−35 28 9.7	14.94	16.60	17.14	44	29	0.382	F351	100	d	
490	0 51 5.5	−33 24 21.4	15.17	18.60	19.25	27	44	0.168	F351	001		
492	0 52 0.3	−31 20 0.5	13.84	17.09	17.86	26	30	0.284	F411	111	d	
493	0 52 41.6	−39 9 32.3	18.25	19.27	19.52	45	77	0.159	F295	001		
494	0 53 24.9	−37 36 35.8	15.35	16.13	17.51	15	7	0.327	F351	110		S 102
495	0 53 28.6	−26 36 9.4	15.86	16.31	17.61	25	8	0.315	F474	223	d	118
496	0 53 32.6	−29 9 31.4	16.58	17.11	17.76	29	31	0.301	F411	100		S 100
497	0 53 41.1	−22 49 56.5	17.11	17.24	18.05	24	23	0.262	F474	100	d	
498	0 53 43.7	−31 48 39.7	16.36	17.37	18.47	21*	24	0.219	F411	001		
499	0 53 51.4	−38 10 2.1	16.62	17.72	18.46	42	33	0.221	F295	011		S 106
500	0 53 59.7	−30 20 2.0	17.92	18.13	18.41	70	56	0.226	F411	111	d	2844
501	0 54 3.3	−24 18 43.5	19.01	19.05	19.83	42*	43	0.140	F475	001		2842
502	0 54 7.4	−27 45 55.0	16.49	17.82	18.71	30	28	0.200	F411	011	d	2843
503	0 54 21.7	−39 2 20.1	16.62	18.76	19.49	65	53	0.155	F295	001		2845
504	0 54 27.5	−22 32 32.9	16.92	17.15	19.05	10	8	0.178	F475	001	d	
505	0 54 38.9	−29 57 0.1	15.92	18.00	0.00	0	0	0.000	F411	110	d	(2846)
506	0 54 39.0	−31 7 10.9	14.87	15.70	17.58	8	5	0.319	F411	111	d	S 109
507	0 54 55.5	−26 33 35.6	16.41	18.17	19.23	19	36	0.168	F475	001	d	122
508	0 55 1.9	−29 58 31.7	18.84	18.90	19.83	26	88	0.138	F411	001	d	
509	0 55 3.0	−29 42 49.4	16.50	17.65	0.00	0	0	0.000	F411	010	d	(S 108)
511	0 55 50.0	−31 17 20.5	17.31	0.00	0.00	0*	0	0.000	F412	001	d	
512	0 56 8.0	−34 34 0.4	13.82	17.17	18.28	32*	19	0.238	F351	111		2847
513	0 56 48.1	−29 19 41.8	17.38	19.45	19.87	78	40	0.137	F412	001		2850
514?	0 57 23.4	−30 39 5.8	16.10	17.69	18.65	21	29	0.204	F412	001		2851
515?	0 58 17.5	−34 58 2.6	17.13	17.35	18.08	37	29	0.259	F351	100		
516	0 58 26.0	−40 30 22.6	13.62	15.68	17.39	12	6	0.345	F295	110		S 113
517	1 0 7.7	−33 36 54.6	16.39	17.23	18.60	20	14	0.195	F352	010		
518	1 0 57.9	−22 51 54.1	19.41	19.51	20.00	45	39	0.134	F475	001		0135
519	1 2 7.7	−40 6 22.4	16.53	17.27	17.97	45	33	0.271	F295	110		2860
520	1 2 11.5	−24 15 37.4	17.32	18.34	18.81	61	46	0.192	F475	011		0140
521	1 2 49.7	−39 14 18.1	15.28	16.13	18.13	8	6	0.254	F295	100		
522	1 3 12.1	−24 55 28.7	19.31	19.33	19.62	55	46	0.149	F475	001		0141
523	1 4 5.6	−33 14 29.0	18.51	18.57	19.95	20	26	0.133	F352	001		
524	1 5 39.9	−37 1 20.6	15.53	18.07	18.64	75	46	0.206	F352	011		2871
525	1 5 40.6	−40 20 12.4	17.03	17.76	18.65	25	31	0.205	F296	010	d	S 127
526	1 6 30.7	−40 37 19.6	16.96	18.21	18.58	88	58	0.210	F296	010	d	2874
527	1 7 42.0	−25 5 2.9	17.19	17.64	18.22	37	28	0.244	F475	111		155
528	1 7 57.7	−30 0 31.6	17.65	17.90	18.81	14	28	0.193	F412	100		2878
529	1 8 5.6	−40 44 52.6	17.61	18.06	0.00	0	0	0.000	F296	100	d	
530	1 10 12.5	−36 37 9.8	16.12	17.77	19.00	27	24	0.181	F352	001		2883
531	1 10 15.7	−35 57 51.4	17.13	19.50	20.09	34	55	0.134	F352	001		
532	1 10 32.1	−33 54 52.1	15.31	16.19	17.43	18	8	0.323	F352	100		
533	1 11 28.1	−32 1 20.5	13.83	0.00	0.00	0*	0	0.000	F412	100	d	(S 141)
534	1 11 30.1	−39 12 20.6	17.07	17.32	18.75	16	19	0.193	F296	001		2885
535	1 11 43.9	−31 59 50.2	12.91	15.04	0.00	0*	0	0.000	F412	011	d	
536	1 12 39.5	−30 4 54.6	15.90	17.15	18.20	15	17	0.246	F412	100		
537	1 13 56.9	−28 37 58.0	18.44	18.84	19.41	39	46	0.151	F412	001		
538	1 14 40.1	−37 19 12.3	15.79	18.10	18.97	31	39	0.178	F352	001		2892

Table 3 – *continued*

EDCC	R.A. h m s	Dec. ° ′ ″	m_1	m_3	m_{10}	n_{clus}	n_{back}	θ_A	Field	runs	Deb.	Abell
539	1 15 16.1	−38 16 27.4	16.68	17.60	18.41	29	36	0.226	F296	112		S 144
540	1 15 55.7	−28 40 46.8	17.10	18.18	19.08	23	34	0.177	F412	010		
541	1 15 55.9	−27 15 13.8	15.93	16.75	17.80	17	13	0.290	F475	111	d	2895
542	1 16 15.4	−26 53 22.9	17.10	17.99	18.46	36*	40	0.220	F475	111	d	
543	1 17 9.3	−36 7 38.6	15.73	16.95	18.69	10	10	0.201	F352	010		
544	1 18 32.1	−30 42 15.6	18.31	18.47	19.03	57	49	0.179	F412	012		S 151
545	1 18 45.5	−31 20 28.4	15.05	16.78	18.85	5	7	0.190	F412	011		
546	1 19 45.7	−39 53 30.0	16.80	17.55	18.39	32	32	0.215	F296	010		
547	1 20 20.4	−33 4 11.8	14.66	17.48	18.43	22*	24	0.221	F352	100		
548	1 21 12.2	−27 17 34.3	16.27	17.16	19.16	8	9	0.169	F476	001		2906
549	1 21 38.4	−41 6 59.9	16.54	16.78	18.32	12	14	0.236	F296	100		
550	1 22 11.8	−37 37 50.7	14.66	17.85	18.78	47*	34	0.195	F352	011	d	2909
551	1 22 42.2	−37 55 40.1	18.35	18.84	19.35	8	66	0.162	F296	010	d	
552	1 22 58.3	−26 21 8.4	17.48	17.61	18.96	19	20	0.183	F476	010		
553	1 23 9.0	−39 41 37.1	16.71	17.47	18.05	55*	41	0.262	F296	110		S 156
554	1 23 9.3	−33 35 11.0	15.07	17.36	19.29	8	13	0.166	F352	001	d	
555	1 23 24.9	−29 48 28.2	16.92	17.56	18.33	35	28	0.233	F413	111		
556	1 23 39.6	−33 46 37.1	16.99	18.09	19.98	11	23	0.133	F353	001	d	2910
557	1 23 46.9	−38 14 34.8	14.33	14.35	17.53	5	1	0.326	F296	111	d	2911
558	1 23 56.2	−40 40 22.9	16.85	17.35	18.60	10	23	0.213	F296	010		
559	1 24 54.7	−35 50 45.1	13.83	15.97	18.58	4*	2	0.203	F353	010		
560	1 25 0.9	−23 1 25.6	15.30	16.18	17.59	12	9	0.317	F476	100		
561	1 25 59.4	−29 14 42.1	15.83	17.16	18.76	14*	13	0.196	F413	011		2915
562	1 26 12.6	−25 54 9.3	19.28	19.29	19.53	35	39	0.148	F476	001		0206
563	1 26 37.6	−34 13 24.4	17.88	18.23	19.54	15	30	0.152	F353	001		(2913)
564	1 27 28.9	−33 9 24.1	14.58	16.22	17.59	13	9	0.317	F353	111		S 160
565	1 29 3.4	−41 27 37.8	14.81	16.53	18.37	9	9	0.231	F296	100		
567	1 29 42.3	−24 59 43.0	16.82	17.33	19.19	8	12	0.170	F476	010		2921
568	1 29 42.7	−35 5 59.9	16.10	19.01	19.37	35	62	0.161	F353	011		(2920)
569	1 29 53.8	−26 15 35.2	15.11	16.98	19.33	2*	7	0.166	F476	001		0210
570	1 30 7.7	−42 24 38.7	15.06	17.33	17.91	39*	36	0.278	F296	120		S 163
571	1 30 15.4	−31 20 3.7	15.65	17.16	18.65	18	14	0.205	F413	011		2923
572	1 30 35.6	−29 48 9.7	19.08	19.26	19.55	38*	59	0.145	F413	001		2922
573	1 30 46.5	−27 11 48.2	16.51	16.92	18.40	27	12	0.227	F476	110		2924
574	1 31 39.5	−32 45 54.1	17.53	19.88	0.00	0	0	0.000	F353	010	d	(S 165)
575	1 31 52.4	−27 47 19.3	16.66	17.05	17.87	35	23	0.283	F476	111	d	2926
576	1 31 54.1	−26 21 39.8	17.04	18.00	18.89	47	31	0.188	F476	001	d	214
577	1 32 11.5	−31 52 49.8	16.14	17.38	18.58	23	19	0.210	F413	010		S 166
578	1 32 16.2	−33 3 18.6	15.05	15.44	17.81	3	2	0.289	F353	110	d	S 167
579	1 32 45.4	−27 43 52.2	0.00	0.00	0.00	0	0	0.000	F476	001	d	(2928)
580	1 32 53.3	−23 44 3.9	17.66	18.38	18.82	41	45	0.191	F476	001		0215
581	1 33 4.1	−25 54 41.8	14.77	16.53	17.11	16	19	0.387	F476	111	d	(0214)
582	1 33 17.2	−22 58 15.9	15.29	16.23	17.54	15	10	0.329	F476	100		
583	1 34 8.8	−36 44 25.8	14.34	17.08	18.91	10	9	0.176	F353	001		
584	1 34 49.8	−34 58 24.4	17.17	18.67	19.45	23	43	0.156	F353	001		2930
585	1 35 25.3	−26 56 16.0	16.53	16.90	19.10	5	7	0.176	F476	011		
586	1 39 26.9	−30 50 23.3	17.75	19.22	19.72	29	62	0.145	F413	001		
587	1 39 46.9	−42 24 57.6	15.44	17.17	17.49	47	34	0.330	F297	110		S 180
588	1 40 37.0	−40 24 35.8	15.15	16.23	18.46	6	4	0.237	F297	100		
589	1 41 10.0	−36 33 30.0	13.91	16.44	18.17	14	7	0.249	F353	100		S 182
590	1 41 34.6	−32 43 30.6	18.74	18.83	19.73	30	49	0.152	F413	001		
591	1 41 46.0	−35 32 50.0	16.81	17.01	17.59	28	25	0.317	F353	111		S 186
592	1 43 8.5	−29 29 23.9	17.79	19.07	20.06	67*	42	0.130	F414	001		
593	1 43 36.3	−29 6 28.6	16.90	17.37	19.26	11	10	0.167	F414	010		S 189
594	1 44 4.6	−32 7 19.5	17.39	18.55	19.35	41	43	0.161	F414	001		
595	1 45 3.8	−40 19 6.8	17.24	17.24	18.91	16	9	0.181	F297	010		
596	1 46 3.8	−32 10 16.6	18.10	18.43	19.14	74	44	0.174	F414	011		2943
597	1 49 3.5	−36 25 28.6	14.27	16.34	18.59	3	4	0.209	F354	011	d	
598	1 49 37.2	−26 3 24.7	16.59	18.43	18.83	53	51	0.192	F477	011		0264
599	1 50 2.9	−36 7 8.7	15.90	16.67	18.45	13*	7	0.222	F354	010	d	
600	1 51 1.7	−33 52 36.5	17.89	18.28	19.33	42	34	0.163	F354	001		S 203
601	1 51 26.0	−33 22 6.1	16.51	17.66	18.77	16	23	0.195	F354	011		
602	1 51 29.8	−26 46 45.0	16.19	18.35	19.21	42	34	0.161	F477	001		2950
603	1 52 2.8	−35 55 56.4	14.81	16.09	18.23	4*	4	0.243	F354	011	d	2952
604	1 54 50.3	−24 14 20.6	18.69	19.17	19.85	26	45	0.137	F477	001		2956
605	1 57 51.6	−31 27 59.8	16.84	18.52	19.73	20	34	0.151	F414	001		2961
606	1 58 27.2	−33 11 15.2	17.19	17.56	17.90	45*	42	0.278	F354	120		2962
607	1 58 49.6	−25 20 34.8	14.14	16.83	19.43	5	4	0.158	F477	001		2964
608	1 58 54.9	−40 39 57.9	16.29	16.76	18.31	22	9	0.236	F298	110		2965
609	1 58 57.8	−36 9 52.1	17.28	17.80	18.46	44	40	0.221	F354	111	d	2963
610	1 59 26.1	−37 15 45.5	18.66	19.01	19.47	22*	60	0.158	F354	001		S 216
611	1 59 43.1	−36 3 14.8	0.00	0.00	0.00	0	0	0.000	F354	001	d	(S 219)
612	1 59 45.4	−35 24 14.9	18.10	18.14	19.12	18	36	0.172	F354	001		
613	1 59 55.2	−25 50 32.6	18.66	19.10	19.73	81	48	0.143	F477	001	d	0297
614	2 0 29.7	−34 31 24.2	17.68	17.74	19.00	33	25	0.181	F354	011		
615	2 0 36.3	−28 31 1.0	17.80	18.23	18.96	21	39	0.183	F414	011		2967
616	2 0 59.0	−25 48 43.8	18.68	18.98	19.71	14	50	0.144	F477	001	d	
617	2 1 19.5	−27 14 52.3	16.50	17.42	17.99	45*	35	0.268	F478	110		2968
618	2 1 28.8	−41 20 44.7	16.86	17.81	18.31	68	44	0.236	F298	110		2969
619	2 2 23.7	−35 55 52.8	17.46	17.95	18.96	43	34	0.187	F354	001		2970
620	2 3 5.4	−32 33 28.2	14.74	17.60	20.13	4	10	0.128	F414	001		
621	2 3 42.9	−27 23 49.4	17.33	17.64	18.77	42	25	0.195	F478	011		2972
622	2 3 51.3	−36 22 22.1	15.37	16.66	17.87	30	14	0.283	F354	100		
623	2 4 12.1	−28 38 46.5	14.89	16.96	17.79	42	22	0.292	F414	110	d	
624?	2 4 43.5	−28 53 16.9	16.53	18.56	19.14	−6	90	0.174	F414	010	d	2975
625	2 5 3.7	−35 56 14.8	14.96	17.41	18.39	24	24	0.216	F354	100		

Table 3 – *continued*

EDCC	R.A. h m s	Dec. ° ′ ″	m_1	m_3	m_{10}	n_{clus}	n_{back}	θ_A	Field	runs	Deb.	Abell
626	2 6 2.8	−32 10 44.5	17.15	18.06	18.48	44*	49	0.219	F414	110		2978
627	2 6 11.2	−28 42 56.7	16.58	17.16	19.65	4*	7	0.147	F415	001	d	
628	2 6 42.1	−26 36 23.6	17.22	18.01	19.26	15	29	0.167	F478	011		2979
629	2 7 12.0	−37 36 40.7	16.49	17.83	18.47	27	43	0.220	F354	011		(S 223)
630	2 8 6.4	−33 55 0.3	18.45	18.63	19.56	48	45	0.152	F354	001		S 227
631	2 8 15.7	−33 14 26.8	13.67	18.45	19.74	20	30	0.137	F354	001		2983
632	2 9 33.9	−40 31 42.1	15.86	17.99	18.73	51	42	0.198	F298	010	d	2984
633	2 10 40.2	−26 23 31.9	17.88	18.48	19.89	26	31	0.136	F478	001		0327
634	2 10 49.9	−25 32 17.6	16.67	19.33	19.59	84	72	0.156	F478	001		0325
635	2 11 4.5	−34 38 6.8	16.10	16.90	19.04	1	7	0.174	F355	001		S 233
636	2 11 29.4	−40 18 56.7	15.91	17.44	17.96	31	37	0.272	F298	100	d	
637	2 12 10.5	−30 46 2.3	16.95	17.25	18.82	14	12	0.187	F415	010		2990
638	2 12 24.3	−26 1 24.2	18.07	18.48	19.55	24	37	0.152	F478	001		2991
639	2 12 48.9	−26 52 58.6	16.10	17.41	19.33	8	12	0.161	F478	001		2992
640	2 12 54.2	−36 47 44.6	18.45	18.56	19.86	32*	33	0.138	F355	001		2993
641	2 13 51.9	−27 46 47.1	17.12	17.40	18.51	21*	23	0.217	F415	011		
642	2 14 8.3	−29 15 17.0	16.87	18.39	19.27	18	45	0.172	F415	001		
643?	2 17 42.1	−28 36 59.4	17.23	18.36	19.03	33	42	0.169	F415	001		S 245
644	2 18 40.9	−26 50 54.5	16.83	17.38	19.31	10	12	0.166	F478	010		
645	2 23 11.7	−29 43 24.8	15.86	16.04	17.14	25	9	0.383	F415	111	d	S 258
646	2 23 27.6	−35 1 26.5	18.23	18.83	19.61	23	43	0.148	F355	010		
647	2 23 50.1	−42 10 29.4	15.49	17.08	18.80	10*	9	0.191	F299	010		3017
648	2 24 8.5	−23 37 36.4	14.61	16.16	18.05	7	6	0.262	F479	100	d	S 263
649	2 24 54.3	−26 43 7.3	15.89	17.44	18.32	43	25	0.235	F479	110		
650	2 24 54.4	−23 8 46.5	15.51	16.28	17.62	13*	9	0.313	F479	100	d	
651	2 24 56.3	−29 4 55.0	17.72	19.25	19.61	79	51	0.140	F415	001		(S 266)
652	2 25 11.6	−29 49 30.8	16.65	16.72	19.13	4*	7	0.174	F415	010	d	
653	2 27 16.9	−33 41 37.0	15.23	16.47	18.09	17	8	0.258	F355	111	d	
654	2 27 52.7	−36 59 52.0	18.75	18.99	19.77	41	46	0.141	F355	001		3026
655	2 28 3.9	−24 49 29.9	17.26	17.40	17.85	36	35	0.283	F479	100		
656	2 28 13.0	−39 8 10.0	17.32	18.98	19.76	34	56	0.141	F299	001	d	S 271
657	2 28 19.7	−32 4 59.7	16.68	17.44	18.38	19	23	0.229	F415	100	d	
658	2 28 34.9	−33 17 55.5	16.26	16.82	17.91	29	15	0.278	F355	111	d	3027
659	2 29 0.5	−38 55 27.1	17.54	18.31	19.28	30	36	0.166	F299	001	d	3029
660	2 29 12.5	−23 5 47.4	15.30	15.85	18.07	6	3	0.260	F479	101		
661?	2 29 59.1	−32 13 26.3	16.65	17.77	18.40	38	32	0.227	F416	100	d	
662	2 30 1.2	−36 55 10.5	14.02	18.81	19.81	39	38	0.140	F355	001		
663	2 30 56.5	−23 22 54.1	17.53	18.63	19.20	33	42	0.170	F479	001		
664	2 31 16.7	−33 4 32.6	15.58	17.46	18.39	18	22	0.224	F355	100		
665	2 32 18.3	−33 52 39.2	14.98	16.32	17.86	11	9	0.284	F355	101		S 278
666	2 32 24.0	−37 42 55.3	15.95	17.18	18.38	14	15	0.229	F299	100		S 279
667	2 32 57.4	−24 44 4.5	17.77	19.75	20.17	31	26	0.124	F479	001		
668	2 33 45.7	−41 58 17.2	17.23	18.03	18.52	36	45	0.214	F299	010		3033
669	2 34 3.7	−22 40 31.2	17.44	18.60	19.11	25	38	0.169	F479	010		
670	2 34 47.0	−24 49 6.8	17.32	17.99	19.05	25	28	0.178	F479	010		
671	2 34 51.9	−25 35 29.7	16.14	17.27	18.20	10	25	0.246	F479	100		
672	2 35 10.9	−26 35 42.5	15.63	16.55	20.07	0	5	0.128	F479	001	d	
673	2 35 23.1	−26 44 13.5	16.45	17.11	19.77	3	11	0.141	F479	101	d	368
675	2 36 6.5	−32 34 12.0	19.26	19.38	19.90	21	47	0.138	F416	001		
676	2 36 7.7	−32 55 2.1	17.10	17.71	19.13	14	20	0.174	F356	010		
677	2 36 25.3	−33 48 47.1	15.13	16.25	18.49	6	5	0.221	F356	010		
678	2 36 48.0	−27 12 5.5	16.65	18.45	19.33	30	37	0.155	F479	001		
679	2 38 58.9	−25 59 37.4	17.14	18.54	19.02	24*	48	0.174	F479	001		
680	2 39 13.0	−28 51 33.9	17.37	18.45	18.89	55	45	0.177	F416	001		3041
681	2 41 29.6	−35 22 55.9	16.50	16.75	18.50	16	11	0.218	F356	110		
682	2 41 31.3	−28 5 8.0	16.77	18.43	19.10	40*	47	0.176	F416	011		3044
683	2 42 26.6	−26 31 10.7	15.78	17.08	17.99	43	25	0.269	F479	112		0380
684	2 42 29.6	−25 7 40.3	17.22	17.75	20.81	2	13	0.101	F479	100	d	
685	2 42 38.5	−28 58 16.2	17.19	17.91	19.21	12	19	0.162	F416	001		(3043)
686	2 43 44.3	−24 55 22.1	14.35	16.67	18.23	11	9	0.243	F479	100	d	
688	2 45 2.6	−42 32 34.1	14.89	16.68	18.21	19	16	0.245	F299	110	d	S 296
689	2 45 14.2	−34 11 48.3	19.05	19.09	19.48	32	54	0.156	F356	001	d	3053
690	2 45 19.2	−27 46 27.8	17.03	17.39	18.32	24	26	0.235	F480	011	d	3052
691	2 45 21.8	−34 55 44.4	16.96	18.52	19.01	34	56	0.189	F356	001		
692	2 45 34.2	−22 51 49.6	14.65	17.22	18.37	15	17	0.229	F480	110		
693	2 45 51.1	−42 3 37.9	16.04	16.69	16.90	24	35	0.422	F299	110	d	S 297
694	2 46 14.7	−27 53 52.0	17.01	18.43	0.00	0*	0	0.000	F416	100	d	(3054)
695	2 46 58.4	−31 23 15.8	14.67	14.75	16.04	16	3	0.706	F416	110		S 301
696	2 48 30.6	−40 33 10.2	17.37	17.85	18.38	27	48	0.229	F299	100		
697	2 48 54.0	−35 13 38.0	14.70	15.51	16.79	12	9	0.442	F356	100	d	
698	2 49 7.4	−35 45 11.6	17.42	19.58	20.18	11	23	0.124	F356	001	d	
699	2 49 17.9	−25 9 1.2	16.25	16.58	18.09	28	11	0.257	F480	111		0389
700	2 49 39.5	−25 47 15.5	15.15	17.39	18.33	42	24	0.233	F480	110	d	
701	2 50 6.1	−36 54 24.9	16.92	18.65	18.98	51*	56	0.182	F356	001		3063
702	2 50 8.9	−25 32 42.3	19.13	19.43	19.87	38	66	0.137	F480	001	d	3062
703	2 50 32.4	−41 23 27.3	17.24	18.08	0.00	0	0	0.000	F300	010	d	
704?	2 50 38.5	−33 5 28.7	16.69	17.27	18.23	23	19	0.232	F356	100		
705	2 50 41.7	−42 28 23.8	17.21	18.00	18.28	28	71	0.238	F300	110		
706	2 51 18.1	−26 46 54.6	16.50	18.01	18.96	22	33	0.186	F480	001		
707	2 51 30.2	−33 41 40.2	15.54	16.81	17.83	27*	20	0.287	F356	111		3064
708	2 51 36.4	−41 24 21.8	16.75	17.52	18.76	22	25	0.196	F300	110	d	S 306
709	2 53 7.9	−35 38 35.0	16.04	16.30	17.68	19	15	0.306	F356	111	d	
710	2 53 42.0	−22 51 29.8	16.59	17.75	18.60	37	25	0.208	F480	011		3069
711	2 54 0.6	−40 30 6.9	18.50	18.88	19.33	40	76	0.171	F300	010		
712	2 54 19.6	−24 55 51.1	16.33	17.65	18.40	34	30	0.226	F480	011		3070
713	2 55 28.3	−35 49 27.5	15.11	16.77	17.81	13	23	0.289	F356	101	d	

Table 3 – *continued*

EDCC	R.A. h m s	Dec. ° ′ ″	m_1	m_3	m_{10}	n_{clus}	n_{back}	θ_A	Field	runs	Deb.	Abell
714	2 56 20.9	−26 46 42.2	18.34	18.45	19.24	27	43	0.172	F480	001		
715?	2 56 26.2	−41 8 4.0	16.72	18.23	18.91	41	54	0.187	F300	010		
716?	2 58 51.3	−36 46 46.4	16.13	16.91	17.66	20	35	0.308	F356	100	d	
717	2 58 55.5	−37 14 56.6	14.88	16.30	17.18	21	26	0.376	F356	110	d	S 316
718	2 58 56.3	−38 22 35.4	16.44	16.67	18.65	9	12	0.205	F300	011		
719	2 58 56.8	−33 24 56.2	16.01	17.22	17.81	12	24	0.270	F356	100		
720	2 59 49.3	−25 31 35.5	15.36	16.59	18.43	8	7	0.229	F480	010		
721	3 1 2.3	−34 27 50.6	17.09	18.19	18.81	21	34	0.182	F357	010		
722	3 1 3.9	−37 7 47.2	16.61	16.76	17.07	58	46	0.394	F357	112	d	(3084)
723	3 2 52.4	−37 47 6.4	16.69	17.08	18.37	9	25	0.230	F300	100		
724	3 3 20.5	−39 17 33.2	13.31	16.45	17.71	20	19	0.302	F300	100	d	
725	3 3 55.0	−38 16 11.0	16.23	17.18	18.12	16	34	0.256	F300	100		
726	3 4 43.0	−39 1 47.3	17.43	18.41	18.64	36	81	0.206	F300	111	d	
727	3 6 2.6	−23 8 22.6	13.94	16.34	18.98*	5	3	0.182	F481	100		
728	3 6 13.3	−36 53 32.2	16.03	16.18	17.30	28	21	0.358	F357	111		3089
729	3 6 15.5	−23 53 8.7	15.78	16.68	17.45	34	18	0.336	F481	111		419
731?	3 7 5.5	−37 45 6.1	17.66	18.14	18.99	23	40	0.177	F300	010		
732	3 7 23.7	−24 43 39.9	15.45	17.50	20.91	3	4	0.097	F481	100		
733	3 8 9.2	−38 29 39.0	17.86	18.06	19.84	9	24	0.140	F300	001		
734	3 8 31.3	−26 17 16.1	17.32	17.35	18.49	19	18	0.219	F481	001		
735	3 9 23.7	−27 5 34.3	17.39	17.70	18.43	2	60	0.224	F481	001	d	3094
736	3 9 42.8	−27 11 11.7	15.79	16.03	17.39	20	8	0.345	F481	110	d	
737	3 10 9.4	−22 33 54.3	17.17	17.62	18.15	25*	28	0.243	F481	100		
739	3 10 41.6	−36 44 10.9	16.66	17.42	19.01	17	20	0.181	F357	010		
742	3 11 52.2	−38 30 34.7	15.21	16.51	17.89	26*	19	0.280	F300	111		3098

EDCC	R.A. h m s	Dec. ° ′ ″	m_1	m_3	m_{10}	n_{clus}	n_{back}	θ_A	Field	runs	Deb.	Abell
743	3 11 54.5	−37 54 39.0	17.82	17.86	20.98	6	8	0.095	F300	100		
744	3 12 14.1	−42 10 39.7	16.68	16.98	18.99	7	11	0.178	F300	010		
745?	3 12 16.8	−32 28 20.6	17.05	17.77	18.62	49	22	0.207	F417	011	d	3101
746?	3 12 44.0	−42 37 55.9	16.44	18.67	19.27	27	58	0.164	F300	010		3105
747	3 13 2.4	−41 21 9.0	16.10	17.25	18.51	14	23	0.217	F300	010	d	
748	3 13 9.5	−29 24 14.2	15.74	16.58	17.25	39	14	0.365	F417	111		S 333
749	3 14 24.6	−37 13 39.9	16.91	18.25	19.96	9	20	0.127	F357	100		
751?	3 14 59.5	−42 12 3.5	17.19	17.40	18.30	29	29	0.229	F300	100		
752	3 15 7.0	−38 24 31.9	16.09	17.56	18.95	18	22	0.180	F301	001		
754	3 16 19.3	−39 18 37.1	17.23	19.11	19.70	69	50	0.143	F301	001		3114
755	3 18 23.9	−24 52 30.0	17.02	18.24	18.99	45*	29	0.181	F481	011		
756	3 18 42.3	−27 21 47.7	16.41	16.48	17.81	21	9	0.289	F481	110		S 340
757	3 19 46.0	−34 28 45.4	17.53	17.99	18.44	48	32	0.223	F357	121		3118
758	3 20 22.1	−41 30 46.8	15.74	16.99	17.55	51	33	0.321	F301	110		3122
759	3 21 23.1	−40 29 4.8	16.34	17.90	20.64	5	10	0.107	F301	100		
761	3 26 4.2	−26 38 15.0	16.73	17.54	18.83	21	7	0.181	F481	001		
762	3 32 15.2	−39 8 9.1	15.78	16.34	17.25	39	14	0.364	F301	110	d	3135
763	3 32 55.2	−39 38 0.9	16.35	17.52	18.36	23	31	0.230	F301	011	d	S 364
764	3 33 22.4	−42 36 8.3	15.45	17.24	18.63	9	15	0.210	F301	010		S 365
765	3 34 50.6	−39 53 15.6	16.01	16.71	17.95	30	15	0.273	F301	110	d	3142
766	3 36 2.3	−38 11 32.8	17.17	18.16	19.18	30	21	0.163	F301	001		3145
767	3 37 7.6	−40 44 57.6	16.67	17.27	18.62	18	18	0.204	F301	010		
768	3 37 55.9	−40 9 58.6	15.74	18.42	18.83	36	61	0.197	F301	010		
769	3 38 34.0	−38 3 8.0	15.56	16.91	18.75	13	7	0.194	F301	010		S 376

Table 4. Objects misidentified as clusters. Gal: galaxy; Star: star(s); s.t.: satellite trail; d.s.: diffraction spike(s).

EDCC	R.A. h	m	s	Dec. °	′	″	m_1	m_3	m_{10}	n_{clus}	n_{back}	θ_A	Field	runs	Deb.	Object
30	21	41	48.8	−30	8	16.9	15.42	16.70	18.21	16	14	0.245	F466	112	d	Gal
41	21	46	10.5	−35	30	51.0	18.04	18.39	18.87	50	42	0.189	F404	100	d	d.s
56	21	52	36.1	−33	14	48.9	16.95	18.19	19.30	17	41	0.164	F404	011		d.s.
63	21	54	3.2	−34	48	23.3	12.89	17.52	18.89	18	25	0.188	F404	010	d	Gal
71	21	56	46.1	−25	58	35.2	15.93	17.26	18.80	19	19	0.193	F532	011		d.s.
74	21	57	57.7	−35	42	4.1	16.03	18.00	19.02	14	39	0.180	F404	111		Star
109	22	9	49.9	−38	25	29.5	14.57	18.39	19.79	10	37	0.140	F344	001	d	Gal
138	22	20	31.3	−42	30	40.4	16.84	18.11	18.72	53	47	0.192	F345	010		Gal
157	22	30	7.8	−24	48	26.6	16.99	18.92	19.24	33	68	0.168	F533	001		Star
167	22	34	14.7	−25	30	13.0	17.42	17.93	19.19	11	28	0.175	F534	001		Gal
193	22	45	38.0	−22	39	24.0	12.31	16.52	17.96	20	9	0.271	F534	100		Gal
233	22	59	32.1	−39	49	40.4	15.71	16.00	17.17	23	16	0.378	F346	110		Gal
238	23	0	5.8	−37	22	15.5	14.16	18.05	18.34	47	70	0.232	F406	100		Gal
280	23	15	59.9	−32	45	7.0	16.73	17.89	18.92	21	31	0.186	F470	011		Star
337	23	40	50.6	−33	21	32.3	17.16	17.37	19.40	7	13	0.158	F408	010		d.s.
340	23	42	3.4	−25	55	45.8	17.44	18.42	19.67	1	37	0.145	F537	100	d	d.s.
364	23	51	37.2	−42	36	30.9	15.85	16.52	18.46	11	7	0.221	F348	100		Star
379	23	56	51.0	−32	29	40.3	0.00	0.00	0.00	0	0	0.000	F471	011	d	Star
467	0	36	27.5	−25	50	54.2	16.31	16.80	18.18	12	17	0.249	F474	110	d	Star
478	0	44	39.9	−38	16	51.1	18.64	18.83	20.05	17	33	0.128	F295	001		Star
491	0	51	32.2	−27	25	13.7	15.18	17.38	19.31	9	13	0.170	F474	001		Gal
510	0	55	18.3	−27	44	59.9	13.15	18.84	19.45	54	57	0.157	F411	001	d	Gal
566	1	29	39.7	−33	22	32.1	16.78	17.43	18.96	12	17	0.185	F353	001		Gal
674	2	35	32.1	−36	22	40.1	16.63	18.61	20.34	11	22	0.117	F355	001		d.s.
687	2	43	45.3	−34	7	13.0	17.07	17.29	17.86	39	35	0.284	F356	110	d	d.s.
730	3	6	52.6	−32	42	34.2	16.52	16.88	17.89	21	16	0.280	F417	101		s.t.
738	3	10	32.3	−32	34	4.2	17.09	17.73	18.59	34	23	0.209	F417	001	d	Star
740	3	10	44.4	−31	40	17.6	16.36	17.39	19.09	11	10	0.176	F417	011		Gal
741	3	11	29.9	−25	23	31.0	15.61	17.63	18.15	9	34	0.252	F481	111		Gal
750	3	14	32.0	−35	45	12.0	15.89	16.53	17.00	60	32	0.405	F357	211		d.s.
753	3	15	21.8	−41	16	36.9	11.10	17.72	18.35	50	41	0.231	F301	110	d	Gal
760	3	22	48.1	−36	32	25.6	11.77	16.50	18.05	14	8	0.262	F357	110		Gal

shown in Fig. 2 has a slope of 0.65, but a value as low as 0.55 or as high as 0.75 cannot be ruled out on the basis of our data alone since only small changes in the numbers of clusters with $b_j < 17$ change the slope significantly. If we were to assume that the ACO classification of the missing bright clusters in terms of richness and magnitude was accurate, then the slope will be more severely constrained around the value of 0.65. It is encouraging that this value is close to the value of 0.6 expected for a homogeneous distribution at low redshift with minimal curvature or K-correction. We also estimate the completeness limit of the EDCC as $m_{10}(b_j) = 18.75$ since beyond this magnitude the differential counts decline. Given that a cluster must have $m_3 + 2 < 20.5$ for it to be found within the EDSGC, this value is in agreement with what is expected. The ACO clusters would appear to have a similar completeness limit, though the nature of the 'completeness' of the ACO catalogue will be discussed further in the next section.

The distribution of the number–richness relation is shown in Fig. 3. There is evidence from this plot for incompleteness in ACO at counts less than 40, since the number of clusters with fewer members declines. The expectation would be that the number should continue to increase at smaller counts. The EDCC is therefore more complete at lower richnesses than the ACO supplementary catalogue, and there is no evidence for incompleteness in the EDCC with richness for counts above zero. An explanation for this is that the ACO counts are generally overestimated. Then incompleteness in the ACO catalogue would only occur for the supplementary clusters, where no claim is made for any rigorous detection of all such clusters. This also agrees with the comparisons between the catalogues outlined below. This plot also shows that the EDCC does not suffer from any 'hidden' incompleteness such as might be expected if the poorer clusters were only found brighter than a certain magnitude, whereas the richer ones were visible to the quoted completeness limit of the EDCC.

Finally, as discussed in Section 2.2, the binning method imposes a selection criterion in terms of the size of the final cluster. The distribution of the Abell radii of the clusters

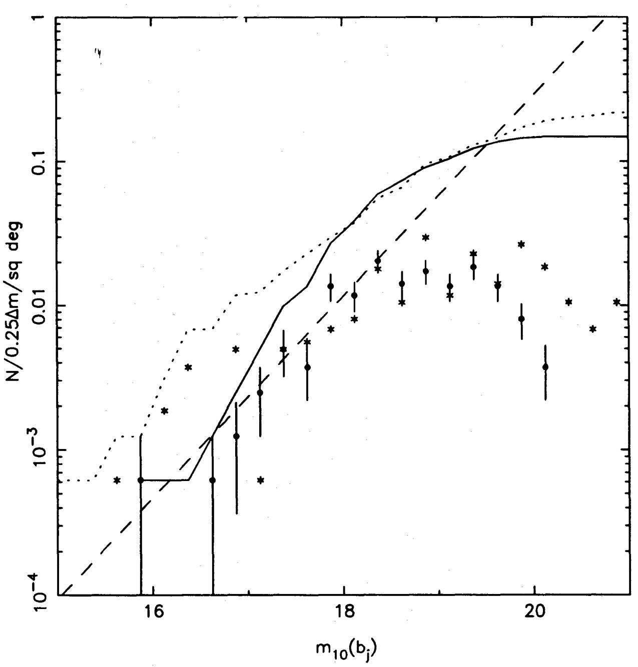

Figure 2. Number–magnitude counts for the EDCC and ACO. Differential counts are indicated by ●(EDCC) and ⋆(ACO). The solid line is the cumulative EDCC counts, and the dotted line the cumulative ACO counts. The dashed straight-line fit has a slope of 0.65 ± 0.05, and is fitted to the EDCC data between $b_j \sim 15.9$ and ~ 18.9. The error bars on the differential EDCC counts are Poissonian.

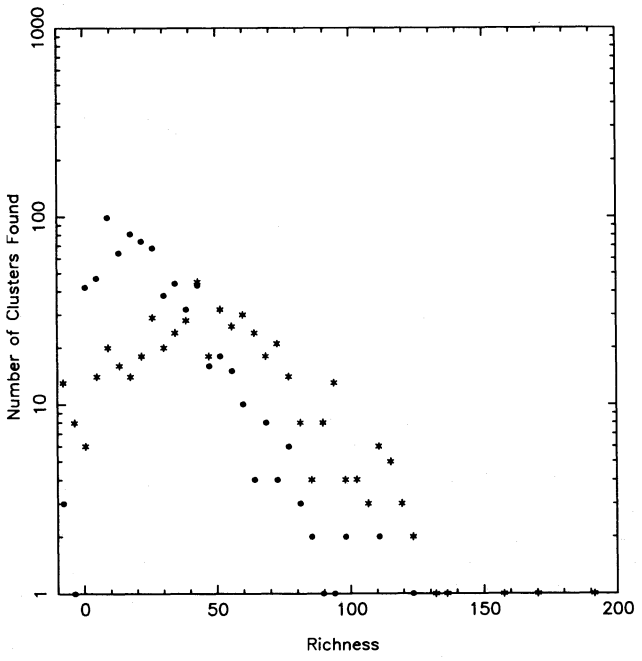

Figure 3. Number–richness counts for the EDCC and ACO. Symbols as in Fig. 2.

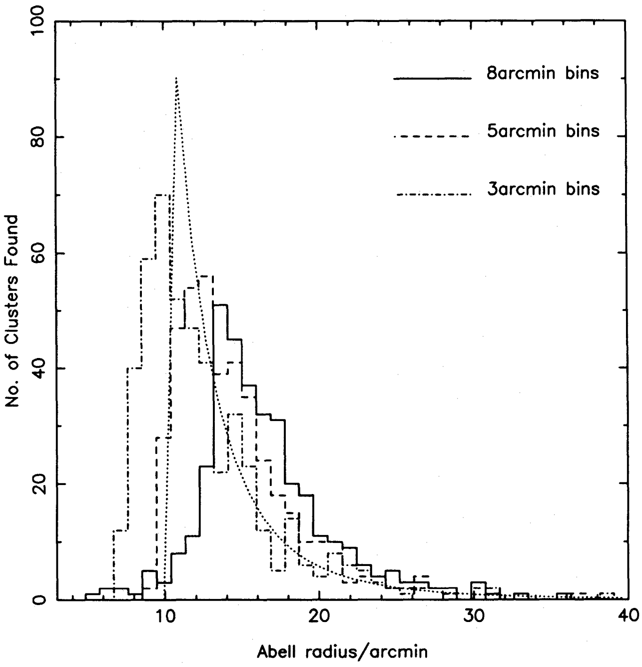

Figure 4. Comparison of the expected size distribution of Abell clusters (dotted line) compared to that found for the EDCC. The expected size distribution of the Abell clusters was calculated assuming a slope for the differential number–magnitude counts of 0.6.

found for the different initial sizes is shown in Fig. 4. Also plotted is the expected number of clusters with a given Abell radius if it was assumed that the number–magnitude distribution for the clusters had a slope of 0.6. Given the uncertainty in the actual slope of the number counts, the agreement between the observed and predicted distribution is another indication that there is no significant problem with the method adopted.

The sky distribution of the clusters is shown in Fig. 5. The clusters follow the general galaxy distribution well. Clusters within areas of low galaxy density are still located where genuine over-densities exist. There is no evidence for any systematic gradients or other effects in this plot. We therefore conclude that the EDCC has no systematic incompleteness with position. A more detailed examination of the structures seen in this plot is given in Guzzo *et al.* (1992).

4 COMPARISON WITH THE ABELL CATALOGUE

4.1 Comparison sample

All the Abell clusters from the 60 EDSGC fields were extracted from the ACO catalogue. These clusters included all the full ACO clusters (restricted to those clusters with richness greater than 30 and distance class less than or equal to 6: see ACO for the definition), all the supplementary ACO clusters, and those clusters that lay within the overlap region between the northern and southern catalogues. There were 339 full ACO clusters, 228 supplementary clusters and 87 within the overlap region. For the latter, both their original Abell (1958) classification (as tabulated by ACO) and the newer southern classifications were considered. In order to carry out the comparison between these clusters and the catalogue presented here, both the V magnitude system of ACO and the R magnitude scale of Abell (1958) were converted to the photographic magnitude b_j. As noted

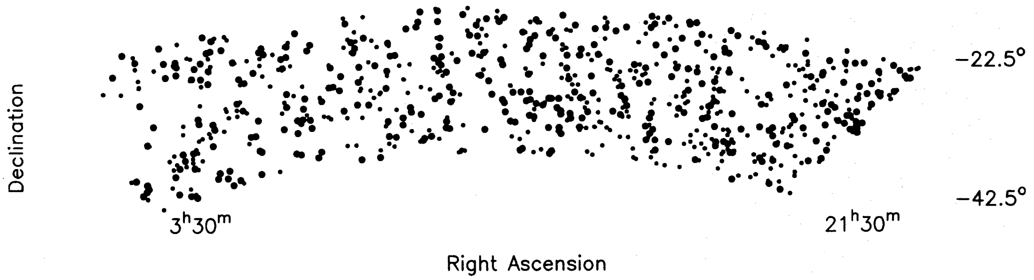

Figure 5. Sky distribution of the EDCC clusters. Large dots have richness > 30, small dots richness < 30.

previously, the relation $b_j - V = 0.77$ was adopted for transforming the raw ACO V magnitudes and a correction given by $b_j - R = 1.07$ was used for the northern clusters, following equation (9) of ACO. We have ignored the extinction corrections applied by Abell to the northern catalogue. This is valid since the measured extinction at the galactic latitudes covered by the EDCC is smaller than the errors within the catalogue.

In order to make a direct comparison between the EDCC and ACO clusters a consistent definition of the Abell parameters must be applied. One aspect of the ACO catalogue which remains very uncertain is the adopted background correction. ACO adopt a global background correction, and then force agreement with the northern Abell catalogue. As noted by ACO themselves, their global background subtraction is not realistic, since it can result in negative counts. Although our aim is to compare directly the selection methods of Abell and EDCC, our information is fully digitized and we can be more flexible in the definition of cluster parameters than ACO. Therefore, we also estimated local background-corrected counts for the ACO clusters by reconstructing their raw counts (using their data and equations 1, 6 and 7 of ACO) and then calculating a new local background count from the EDSGC data. Only richness and magnitude comparisons are presented here. Comparisons with the more subjective parameters (e.g. classification of the cluster shape) quoted in ACO were not carried out.

4.2 The comparison

As described above, all the Abell clusters within the EDCC area were used in the comparison, plus those within 20 arcmin of the boundary. A match occurred when both the EDCC cluster centroid and the Abell cluster centroid lay within the other's Abell radius. Only one match was allowed per cluster. Those EDCC clusters that had fewer than 10 members after deblending were excluded (because of the impossibility of comparing magnitudes) but those ACO clusters with fewer than 10 members were included (since ACO still quote magnitudes for these clusters). In all, there were 308 matches between the combined ACO plus overlap catalogue and the EDCC.

As a test of the reliability of the comparison a maximum allowed offset, beyond which no matches were allowed, was considered. This did not seriously affect the scatter between the Abell and EDCC catalogues but did change the matching percentages. Table 5 gives values of the calculated scatter for both the complete comparison and this restricted set. This

Table 5. Comparison of EDCC and Abell catalogues.

Sample	σ_{m_1}	σ_{m_3}	$\sigma_{m_{10}}$	σ_{counts}
All ACO clusters	1.30	0.93	0.79	34.7
ACO clusters with offset < 5′	1.21	0.88	0.74	34.4
Full ACO clusters only	1.34	0.90	0.72	36.7
All Northern clusters			0.78	40.4

included 58 matches with clusters in the overlap region. When a maximum radius of 5 arcmin was imposed, the number of matches was reduced to 243. Since the average offset is 3 arcmin, and the distribution of the offsets is approximately Gaussian, this change in the number of matches is not surprising. If more than one match was allowed per cluster, then an extra nine clusters were detected from the full ACO and northern catalogues. Therefore, the condition that any one EDCC cluster can only match one ACO cluster is valid.

Scatter plots for Abell richness against EDCC richness, and the correlation between Abell m_{10} and EDCC m_{10} are shown in Figs 6 and 7 respectively. The data are shown separately for the northern clusters, and for those classified by Olowin or Corwin. There are no clusters in the ACO sample classified by Abell. The ACO and northern magnitudes have been corrected to b_j using the relation given earlier. For clusters lying in the overlap region of the northern and southern catalogues both classifications have been plotted.

The obvious conclusion from Fig. 6 is the lack of any strong correlation between the richness values (though there is a weak correlation in the expected sense of overall ACO richness being proportional to ours). This is also true when the local background-corrected ACO counts are used and so this lack of correlation reflects a real difference between the catalogues. In addition, there is a systematic tendency for the ACO clusters to have higher richnesses. This seems to be particularly reflected in the northern counts and Corwin's ACO southern counts. Given the steep dependence of the number–richness counts shown in Fig. 3, this explains the apparent greater number of Abell clusters with counts greater than 30 compared to the EDCC (467 as opposed to 249). It is important to stress that this lack of correlation between our richnesses and theirs applies to all clusters. We find all bar five of the 'statistical sample' of Abell (distance class less than or equal to 4 and more than 50 members). However, of those we find, only one third have more than 30

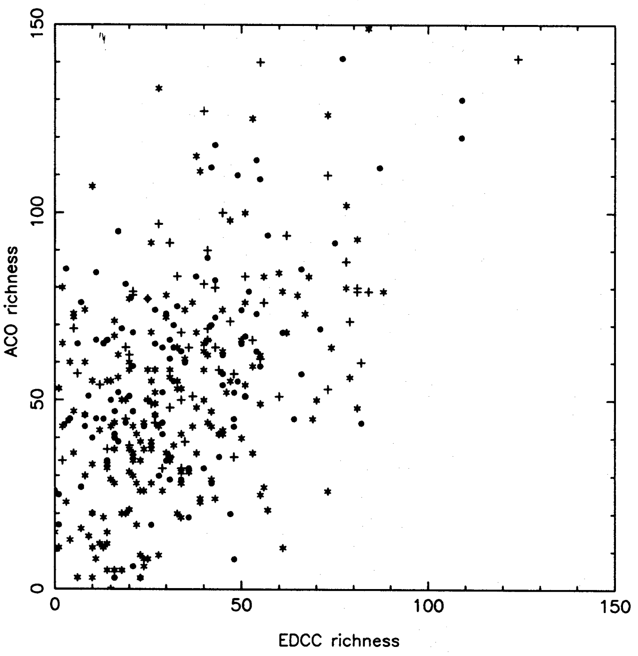

Figure 6. Comparison of the richnesses for clusters found in common between the EDCC and Abell catalogues. ● denotes a Corwin cluster, * an Olowin cluster, and + a northern Abell catalogue cluster.

members and only one sixth more than 50. Clearly, even this sample is prone to a large scatter, sufficient to move the clusters more than one richness class. This is contrary to the analysis of Struble & Rood (1991) who attempt an internal analysis of the Abell catalogues, and must also place in doubt clustering statistics derived from such samples (see Postman, Geller & Huchra 1992).

The magnitude differences between the EDCC and the ACO clusters can best be characterized by the straight-line fit shown in Fig. 7 (though the scatter about this is large, $\sigma \sim 0.7$):

$$m_{10}(\mathrm{EDCC}) - m_{10}(\mathrm{ACO}, b_\mathrm{j}) = 0.31 + 0.03(m_{10}(\mathrm{EDCC}) - 18). \quad (2)$$

This is effectively consistent with a slight constant offset in the ACO clusters. By comparison, the faint northern Abell clusters ($R > 17$) shown in Fig. 7 follow a slope close to 45° indicating that they have almost no dependence on true magnitude. As noted by ACO, they all have magnitudes near $R \sim 17$ regardless of their correct magnitude, a value defined largely by the limit of the Palomar Sky Survey plates. This also explains the reason why so many clusters with $z > 0.2$ (the nominal redshift limit of the Abell catalogue) were detected by Abell, since the m_{10} – cz relation breaks down for northern catalogue clusters with true magnitudes fainter than $R \sim 17$. This difference in the magnitudes between the catalogues is also partially responsible for the much greater richnesses found in ACO. Since a change in magnitude of 0.25 is approximately equivalent to changing the Abell radius by 2 arcmin at $b_\mathrm{j} = 17$, and the Abell radius is 20 arcmin, the change in the counting area is 20 per cent. Therefore, we would expect to see greater richnesses in ACO from this argument.

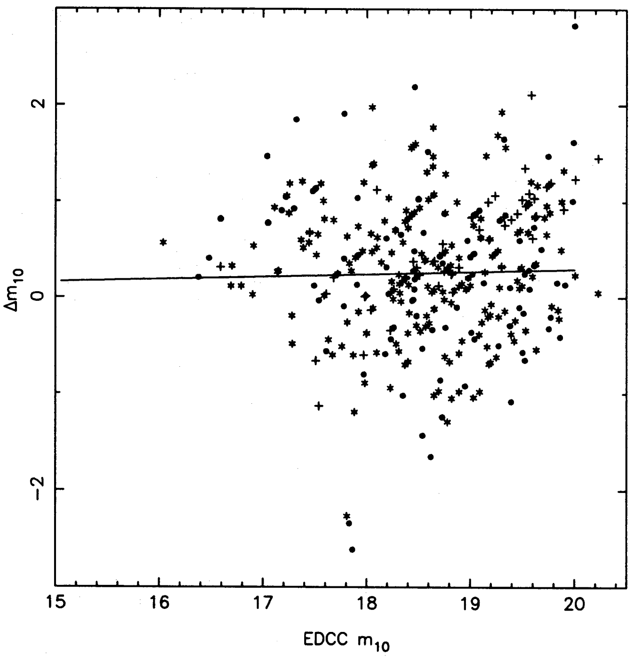

Figure 7. As for Fig. 6 except for m_{10} values. ACO V magnitudes and northern R magnitudes have been corrected to b_j.

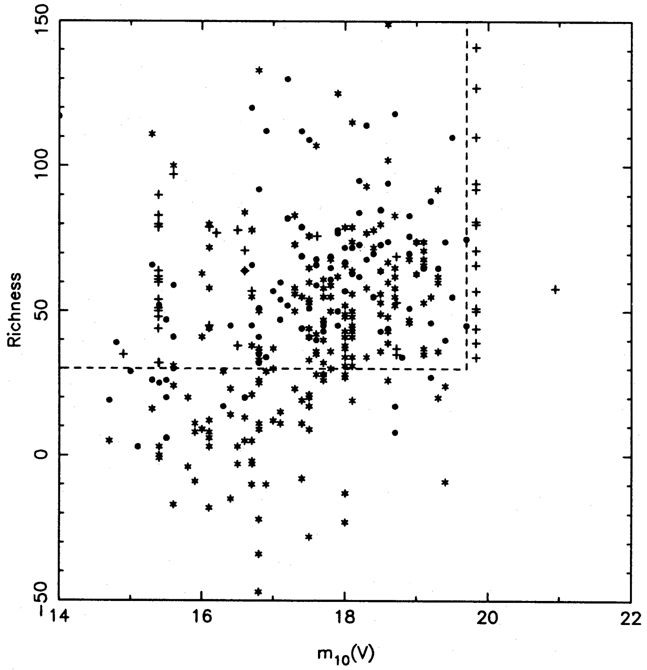

Figure 8. Scatter plot of m_{10} against richness for all those Abell clusters that match up with the EDCC. The dashed lines show the limits of the supplementary catalogue. Symbols as in Fig. 6.

For the full ACO cluster list only, the number of matches found was 222 out of 416 (185 out of 416 for the 5-arcmin matching radius). Therefore, the percentage of full clusters found is 53 per cent and of the supplementary clusters, 36 per cent. Fig. 8 shows a scatter plot of m_{10} against richness for those clusters detected which are in common between the EDCC and Abell catalogues, Fig. 9 shows a plot of those Abell clusters not found, and Fig. 10 a plot of those EDCC

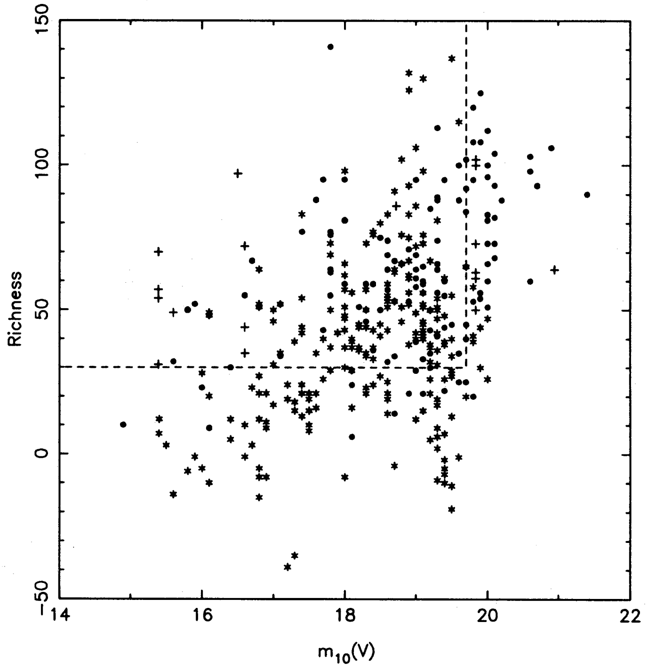

Figure 9. As for Fig. 8 except for those clusters in the Abell catalogue that do not match up with the EDCC. Symbols as in Fig. 6.

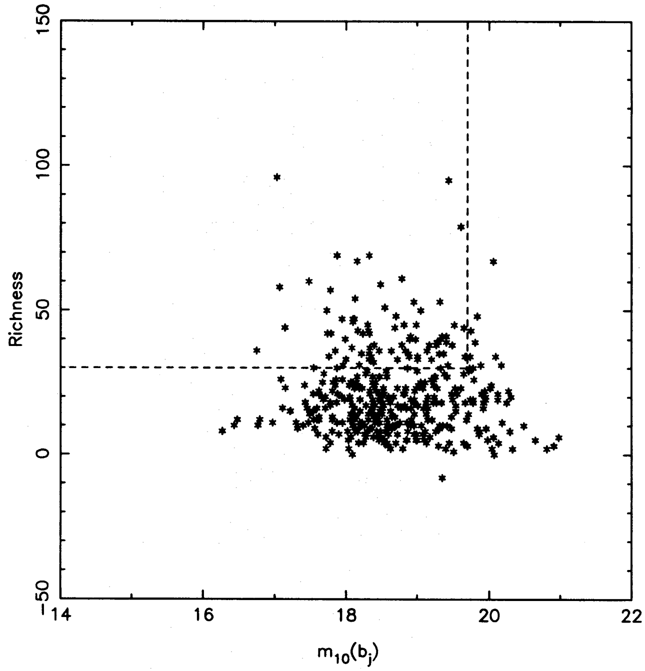

Figure 10. As for Fig. 9 except for those clusters in the EDCC that do not match up with the Abell catalogue. * denotes an EDCC cluster.

clusters not found within the Abell catalogue. The magnitudes of the northern clusters have been transformed into the V band using equations (8) and (9) of ACO. Since the magnitude scale is unreliable beyond $R \sim 17$, it is not surprising that this transformation leaves many northern clusters fainter than $V \sim 20$. The supplementary catalogue limits are marked as dashed lines. In Figs 8 and 9 the values plotted for magnitude and richness are taken from ACO [using their corrected richness but uncorrected $m_{10}(V)$ data].

Fig. 11 shows the percentage of ACO clusters found to any given magnitude within four richness bands. At the nominal completeness limit of the ACO catalogue ($V \sim 17$), 70 per cent of the rich ACO clusters are found within the EDCC. All bar two of the bright ($V<16$) rich clusters are found. In total, 65 per cent of all ACO clusters brighter than the completeness limit of the ACO catalogue are located within the EDCC. Within the completeness limit of the EDCC (assumed to be $V \sim 18$), 80 per cent of the full ACO cluster list are still found (though the rate of detections is dropping rapidly at the limit as shown in Fig. 11). Many of the Abell clusters are considerably fainter in the EDCC survey (since if the EDCC clusters are restricted to $b_j \sim 17.75$ and this comparison carried out again, then only 30 per cent of the ACO clusters are found and 38 per cent of the northern clusters). This is consistent with the relation between the ACO and EDCC magnitude systems derived above. However, the overall detection rates for all clusters only drop sharply for magnitudes fainter than the completeness limit of the EDCC. The overall detection rate of the northern clusters is 70 per cent. This rate does not vary strongly with magnitude given the problems with the northern Abell magnitude system.

By comparison, truncating the EDCC at our completeness limit and comparing with the total ACO catalogue results in only 42 per cent of the EDCC clusters being found. Even if

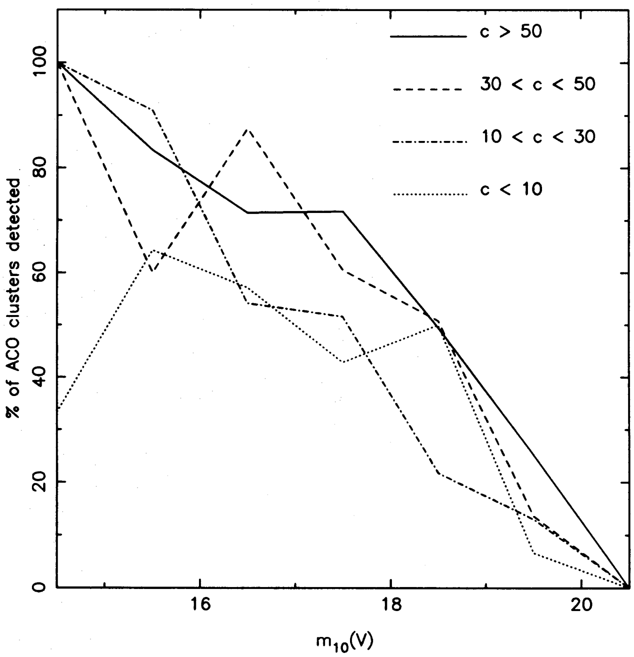

Figure 11. The detection rate of ACO clusters with different richnesses (where richness is denoted by c). The data have been binned into 1 mag wide bins.

only clusters with more than 30 members within the EDCC are considered, this value only rises to 58 per cent. Clearly, there are many more new clusters in the EDCC that are not in the Abell catalogue.

We have visually checked all those missing ACO clusters with $n_{clus}>30$ and distance class less than 5 (see table 2A of ACO for the definition of distance class – the limit corresponds approximately to 17.9 in V for clusters near the SGP). Most of these are either close to the threshold used in the peak-finding algorithm (Section 2.2) or distant. Some of those clusters examined are near areas removed from the EDSGC (satellite trails or bright stars near the centre of the cluster field), or were found to be marginal detections (in terms of finding a peak above the local background). Others also appear to have wildly inaccurate magnitude estimates and may actually lie outside the completeness limit of the EDSGC. In a few cases, no cluster was evident on the plate.

The richnesses for the ACO clusters were also corrected to a local background as described above and a second comparison carried out. This is shown in Table 6. Corwin has systematically larger richnesses (as in Fig. 6 for the global background: a fact they note themselves in ACO in their internal comparisons), whereas for Olowin's clusters the scatter has no systematic trend. The large scatter still found in the richness after correcting to local background counts is partly due to the difficulties of transforming from b_j counts to V counts; however, it is likely that much of the error arises from the quoted errors both for the EDCC and the ACO catalogues (which predict a scatter of about 23 counts – the residual discrepancy between this value and that given in Table 6 is probably due to the difficulties in background estimation). The difficulty in estimating richness for a purely visual survey such as ACO should not be underestimated (see also Scaramella *et al.* 1990, for a discussion of the richness of ACO clusters).

There are also indications that the Corwin clusters have larger true scatters in their magnitude estimates. The scatter is larger than might be expected purely from the quoted errors in the ACO and EDCC surveys. One might expect, for example, a scatter of 0.35 mag for the m_{10} comparison from the estimates of Table 5. Even allowing for a large intrinsic scatter in the galaxies' colours, the $b_j - V$ correction cannot explain the observed discrepancy. However, this may be partly due to chance, since the actual distribution of the most outlying points on the scatter diagram for the Abell/Corwin clusters is mostly the same as that for the Olowin clusters. Part of the scatter in m_{10} probably arises from the difference in definition of m_{10} between ACO and the methods presented here (especially the iterative background-removal procedure). Table 7 gives our final estimates of the internal errors in the ACO catalogue from the comparison carried out above.

5 CONCLUSIONS

The EDCC is the first automated, objectively selected cluster catalogue. Its success rate in finding 80 per cent of the full Abell clusters in the ACO catalogue suggests that, within the quoted completeness limit, the EDCC is at least 90 per cent complete for the Abell subsample (assuming that 10 per cent of all Abell clusters are seriously in error in their classification, as appears to be the case from the visual check carried out of those bright ACO clusters not found in the EDCC as described in Section 4.2). By comparison, almost 70 per cent of the clusters in the EDCC brighter than the completeness limit of $m_{10}(b_j) \sim 18.75$ are new clusters. This lends credence to the idea (already stated by both Abell and ACO) that the Abell catalogue is not useful as a statistical data base.

Furthermore, we find magnitude and richness errors in the Abell catalogues which are sufficient to move such clusters by more than one richness or distance class (in terms of their Abell (1958) definition). This clearly makes the Abell catalogue unsuitable for calculating any large-scale clustering properties. In contrast, the EDCC is statistically complete within the limits and for the selection procedures described.

The extent of the data available will also allow tests of non-Abell classification schemes, or of modifications to the Abell classification scheme (e.g. Sutherland 1989; McGill & Couchman 1990). This will be discussed in detail in a future paper. In order to utilize this new catalogue to its fullest extent, we have also undertaken a large redshift survey programme, using a slightly modified Abell method for our selection. 100 of the richest clusters with $m_{10} < 18.75$ have been observed. On average, 10 redshifts per cluster were obtained. This will enable a rigorous determination of the spatial correlation function (Nichol *et al.* 1992), free from many of the contaminating projection effects notable in previous estimations (e.g. Bahcall & Soneira 1983). The wealth of redshift information will also enable a major analysis of the cluster LF. Since the EDCC covers 5 per cent of the whole sky, it will allow advances in the statistical study of clusters. All these aspects of the catalogue will also be discussed in future papers.

Table 6. Comparison of EDCC and Olowin and Corwin clusters.

Sample	σ_{m_1}	σ_{m_3}	$\sigma_{m_{10}}$	σ_{counts}(local)
Olowin's clusters (local counts)	1.24	0.87	0.56	38.7
Corwin's clusters (local counts)	1.55	1.26	0.98	50.6

Table 7. Estimates of the internal errors in the ACO catalogue.

Sample	σ_{m_1}	σ_{m_3}	$\sigma_{m_{10}}$	σ_{counts}
All clusters	1.28	0.98	0.82	33.0

ACKNOWLEDGMENTS

We would like to thank Harvey MacGillivray for his comments on an early draft of this paper, and the anonymous referee for valuable comments which helped us to clarify the text. We would also like to thank Neil Heydon-Dumbleton for his contributions to the early stages of this project. RCN thanks Roberto Scaramella for enlightening discussions. SLL is grateful to the Royal Observatory, Edinburgh for providing the facilities with which much of this work was carried out and would like to thank Bob Joseph for allowing him to carry on the work at Imperial College. SLL acknowledges receipt of an SERC postdoctoral fellowship during the latter stages of this work and RCN acknowledges receipt of an SERC studentship.

REFERENCES

Aaronson, M., Bothun, G., Mould, J., Huchra, J., Schommer, R. A. & Cornell, M. E., 1986. *Astrophys. J.*, **302**, 536.
Abell, G. O., 1958. *Astrophys. J. Suppl.*, **3**, 211.
Abell, G. O., 1962. In: *Problems of Extragalactic Research, IAU Symp. No. 15*, p. 213, ed. McVittie, G. C., Macmillan, New York.
Abell, G. O., Corwin, H. G. & Olowin, R. P., 1989. *Astrophys. J. Suppl.*, **70**, 1.

Bahcall, N. A. & Soneira, R. M., 1983. *Astrophys. J.,* **270,** 20.
Beard, S. M., MacGillivray, H. T. & Thanisch, P. F., 1990. *Mon. Not. R. astr. Soc.,* **247,** 311.
Colless, M., 1989. *Mon. Not. R. astr. Soc.,* **237,** 799.
Couchman, H. M. P., McGill, C. & Olowin, R. P., 1989. *Mon. Not. R. astr. Soc.,* **239,** 513.
Dodd, R. J. & MacGillivray, H. T., 1986. *Astr. J.,* **92,** 706.
Dressler, A., 1978. *Astrophys. J.,* **223,** 765.
Ellis, R. S., 1990. In: *Gravitational Lenses,* p. 236, eds Mellier, Y., Fort, B. & Soucail, G., Springer-Verlag, Berlin.
Guzzo, L., Nichol, R. C., Collins, C. A. & Lumsden, S. L., 1992. *Astrophys. J. Lett.,* **393,** L5.
Heydon-Dumbleton, N. H., Collins, C. A. & MacGillivray, H. T., 1989. *Mon. Not. R. astr. Soc.,* **238,** 379.
Lucey, J. R., 1983. *Mon. Not. R. astr. Soc.,* **204,** 33.
Lugger, P. M., 1986. *Astrophys. J.,* **303,** 535.
Lynden-Bell, D., Faber, S. M., Burstein, D., Davies, R. L., Dressler, A., Terlevich, R. J. & Wegner, G., 1988. *Astrophys. J.,* **326,** 19.
McGill, C. & Couchman, H. M. P., 1990. *Astrophys. J.,* **364,** 426.
Nichol, R. C., Collins, C. A., Guzzo, L. & Lumsden, S. L., 1992. *Mon. Not. R. astr. Soc.,* **255,** 21P.
Postman, M., Geller, M. J. & Huchra, J. P., 1986. *Astr. J.,* **91,** 1267.
Postman, M., Geller, M. J. & Huchra, J. P., 1992. *Astrophys. J.,* **384,** 404.
Scaramella, R., Zamorani, G., Vettolani, G. & Chincarini, G., 1990. Preprint.
Schechter, P. & Press, W. H., 1976. *Astrophys. J.,* **203,** 557.
Shane, C. D. & Wirtanen, C. A., 1967. *Publs Lick Obs. Bull.,* No. 22, Part 1.
Shectman, S. A., 1985. *Astrophys. J. Suppl.,* **57,** 77.
Struble, M. F. & Rood, H. J., 1991. *Astrophys. J.,* **374,** 395.
Sutherland, W., 1988. *Mon. Not. R. astr. Soc.,* **234,** 159.
Sutherland, W., 1989. *PhD thesis,* University of Cambridge.
Thanisch, P., McNally, B. V. & Robin, A., 1984. *Image Vis. Comp.,* **2,** 4.
Zwicky, F., Herzog, E., Wild, P., Karpowicz, M. & Kowal, C. T., 1961–68. *Catalogue of Galaxies & Clusters of Galaxies,* 6 volumes, California Institute of Technology, Pasadena.